

Electronic Supporting Information

Dichotomy of π -Stacking-Directing Noncovalent Forces in Inorganic–Organic Planar Assemblies. The Case of Platinum(II) Square-Plane π -Stacked with Halo-Substituted Benzoquinones

Eugene A. Katlenok,^{*1} Anton V. Rozhkov,¹ Maxim L. Kuznetsov,² Vitalii V. Suslonov^{1,3}, Vadim Yu. Kukushkin^{*1,4}

¹*Institute of Chemistry, Saint Petersburg State University, Universitetskaya Nab. 7/9, 199034 Saint Petersburg, Russian Federation; e-mails: e.katlenok@spbu.ru, v.kukushkin@spbu.ru*

²*Centro de Química Estrutural, Instituto of Molecular Sciences, Departamento de Engenharia Química, Instituto Superior Técnico, Universidade de Lisboa, Av. Rovisco Pais, 1049–001 Lisboa, Portugal*

³*S.M. Kirov Medical Academy, Akad. Lebedeva St. 6, 194044 Saint Petersburg, Russian Federation*

⁴*Institute of Chemistry and Pharmaceutical Technologies, Altai State University, 656049 Barnaul, Russian Federation*

Table of Contents

S1. CRYSTAL DATA AND STRUCTURE REFINEMENT	3
S2. THERMOGRAVIMETRIC ANALYSIS	15
S3. SOLID-STATE ^{195}Pt NMR SPECTRA	16
S4. CALCULATION DETAILS.....	23
S5. CARTESIAN COORDINATES FOR THE STUDIED MOLECULES.....	42
Optimized geometries.....	42
Cartesian coordinate for $[1\cdot\text{QF}]$ (in Å).....	42
Cartesian coordinate for $[1\cdot\text{QCl}]$ (in Å)	43
Cartesian coordinate for $[1\cdot\text{QBr}]$ (in Å)	44
Cartesian coordinate for $[1\cdot\text{QI}]$ (in Å).....	46
Cartesian coordinate for $[1\cdot(\text{QF})_2]$ (in Å)	48
Cartesian coordinate for $[1\cdot(\text{QCl})_2]$ (in Å).....	49
Cartesian coordinate for $[1\cdot(\text{QBr})_2]$ (in Å)	51
Cartesian coordinate for $[1\cdot(\text{QI})_2]$ (in Å)	52
Cartesian coordinate for 1 (in Å).....	54
Cartesian coordinate for QF (in Å).....	55
Cartesian coordinate for QCl (in Å)	55
Cartesian coordinate for QBr (in Å).....	55
Cartesian coordinate for QI (in Å).....	56

S1. CRYSTAL DATA AND STRUCTURE REFINEMENT

Table S1. Crystal data and structure refinement for **1·QF**, **1·QCl**, **1·QBr**, and **1·QI**.

	1·QF	1·QCl	1·QBr	1·QI
Empirical formula	C ₂₄ H ₁₂ F ₄ N ₂ O ₃ PtS ₂	C ₂₄ H ₁₂ Cl ₄ N ₂ O ₃ PtS ₂	C ₂₄ H ₁₂ Br ₄ N ₂ O ₃ PtS ₂	C ₂₄ H ₁₂ I ₄ N ₂ O ₃ PtS ₂
Formula weight	711.57	777.37	955.21	1143.17
Temperature/K	100(2)	100(2)	100(2)	100(2)
Crystal system	triclinic	monoclinic	monoclinic	orthorhombic
Space group	P-1	P2 ₁	P2 ₁	Pna2 ₁
a/Å	7.30130(10)	7.94224(9)	7.69860(10)	18.1811(3)
b/Å	8.15735(11)	18.6997(2)	17.1871(2)	8.19870(10)
c/Å	18.77600(17)	8.20079(9)	9.55470(10)	17.8672(3)
α/°	101.8971(10)	90	90	90
β/°	92.8080(9)	101.1165(11)	101.2610(10)	90
γ/°	101.3060(11)	90	90	90
Volume/Å ³	1068.36(2)	1195.11(2)	1239.91(3)	2663.31(7)
Z	2	2	2	4
ρ _{calc} g/cm ³	2.212	2.160	2.559	2.851
μ/mm ⁻¹	14.743	17.023	19.996	47.995
F(000)	680.0	744.0	888.0	2064.0
Crystal size/mm ³	0.08 × 0.06 × 0.05	0.15 × 0.1 × 0.1	0.16 × 0.14 × 0.12	0.07 × 0.06 × 0.05
Radiation	CuKα (λ = 1.54184)	CuKα (λ = 1.54184)	CuKα (λ = 1.54184)	Cu Kα (λ = 1.54184)
2Θ range for data collection/°	4.83 to 139.934	9.46 to 139.66	9.438 to 139.998	9.73 to 139.994
Index ranges	-8 ≤ h ≤ 8, -9 ≤ k ≤ 9, -22 ≤ l ≤ 22	-9 ≤ h ≤ 9, -22 ≤ k ≤ 22, -9 ≤ l ≤ 9	-9 ≤ h ≤ 9, -20 ≤ k ≤ 20, -11 ≤ l ≤ 11	-22 ≤ h ≤ 16, -9 ≤ k ≤ 5, -21 ≤ l ≤ 20
Reflections collected	25786	24743	17227	15387
Independent reflections	4019 [R _{int} = 0.0557, R _{sigma} = 0.0316]	4402 [R _{int} = 0.0502, R _{sigma} = 0.0319]	4691 [R _{int} = 0.0458, R _{sigma} = 0.0436]	4529 [R _{int} = 0.0447, R _{sigma} = 0.0380]
Data/restraints/parameters	4019/0/325	4402/1/325	4691/1/325	4529/1/325
Goodness-of-fit on F ²	1.044	1.124	1.076	1.052
Final R indexes [I>=2σ(I)]	R ₁ = 0.0216, wR ₂ = 0.0509	R ₁ = 0.0312, wR ₂ = 0.0814	R ₁ = 0.0222, wR ₂ = 0.0515	R ₁ = 0.0278, wR ₂ = 0.0708
Final R indexes [all data]	R ₁ = 0.0234, wR ₂ = 0.0516	R ₁ = 0.0322, wR ₂ = 0.0820	R ₁ = 0.0229, wR ₂ = 0.0518	R ₁ = 0.0285, wR ₂ = 0.0712
Largest diff. peak/hole / e Å ⁻³	0.98/-0.70	2.49/-1.28	0.80/-0.61	0.86/-0.78

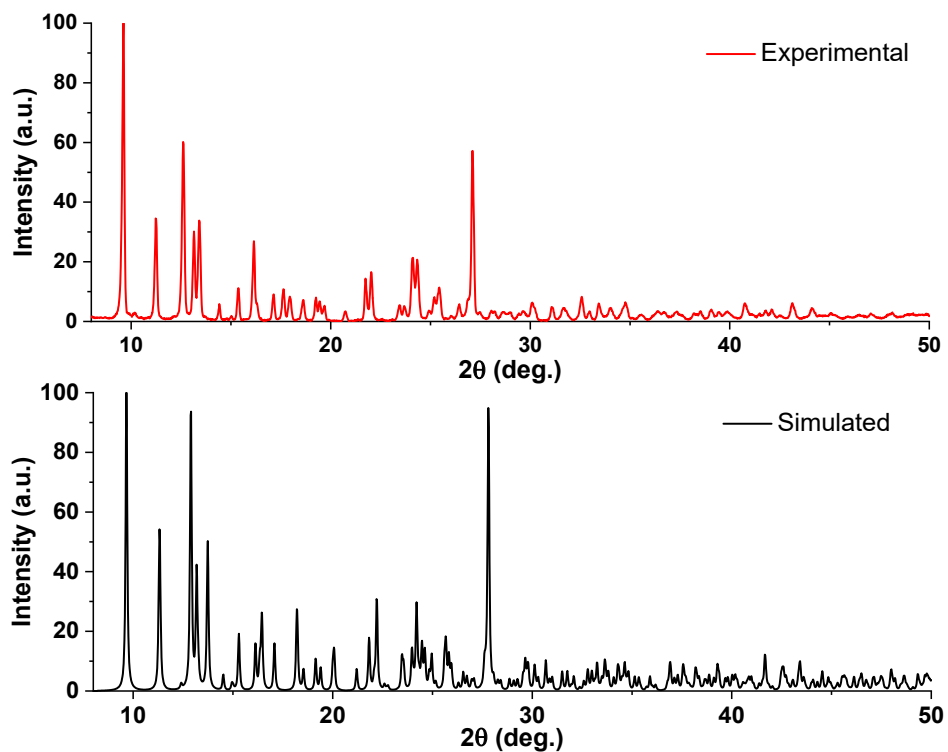


Figure S1. Powder XRD patterns of **1**·QF.

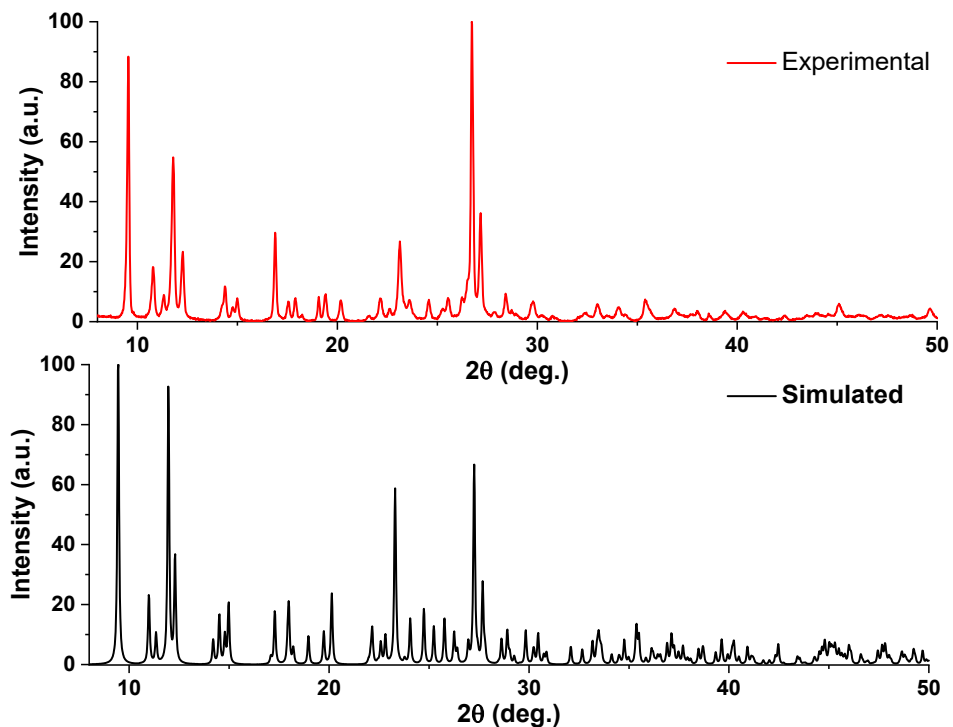


Figure S2. Powder XRD patterns of **1**·QCl.

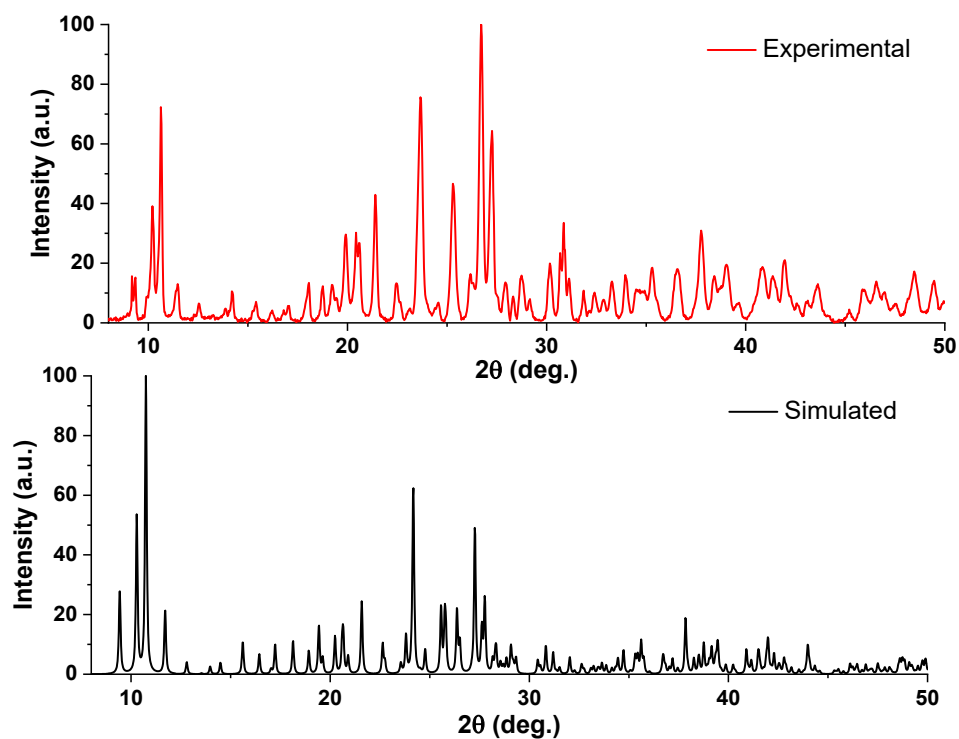


Figure S3. Powder XRD patterns of **1**·QBr.

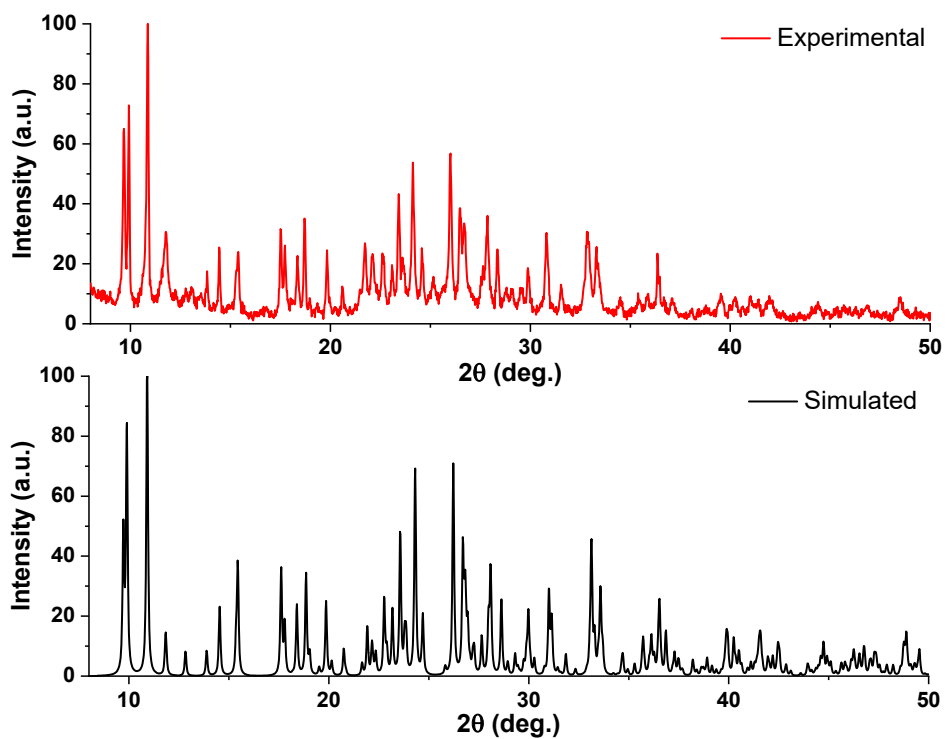


Figure S4. Powder XRD patterns of **1**·QI.

Table S2. Refined unit cell parameters at room temperature from PXRD and cell parameters at 100 K from single-crystal XRD (in square brackets).

	1·QF	1·QCl	1·QBr	1·QI
a, Å	7.4536(10) [7.3013(1)]	8.0004(10) [7.94224(9)]	7.835(3) [7.6986(1)]	18.429(2) [18.1811(3)]
b, Å	8.1791(9) [8.15735(11)]	18.694(2) [18.6997(2)]	17.199(6) [17.1871(2)]	8.2841(9) [8.1987(1)]
c, Å	18.921(2) [18.77600(1)]	8.3850(11) [8.20079(9)]	9.641(3) [9.5547(1)]	17.9630(18) [17.8672(3)]
α , °	101.519(7) [101.8971(10)]	90 [90]	90 [90]	90 [90]
β , °	93.177(5) [92.8080(9)]	99.822(7) [101.1165(11)]	101.816(15) [101.261(1)]	90 [90]
γ , °	99.172(5) [101.3060(11)]	90 [90]	90 [90]	90 [90]

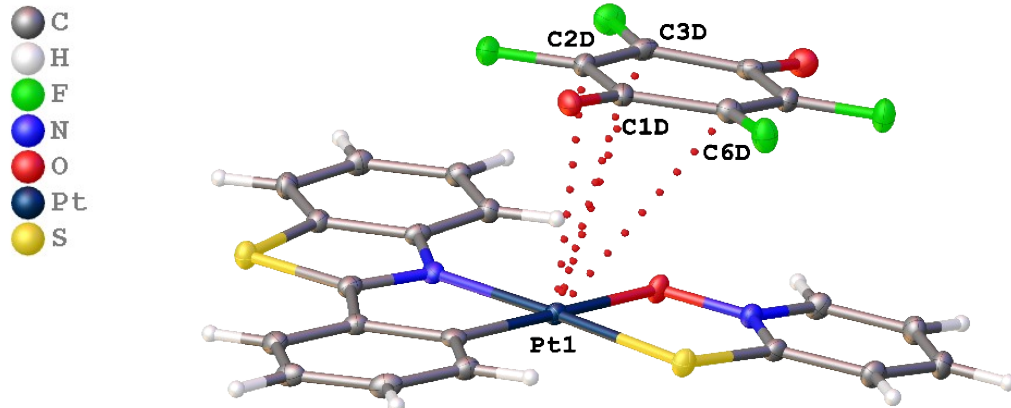


Figure S5. Molecular structure of 1·QF showing C···Pt contacts (dotted lines). Here and in after non-hydrogen atoms are given as probability ellipsoids of atomic displacements ($p = 0.5$).

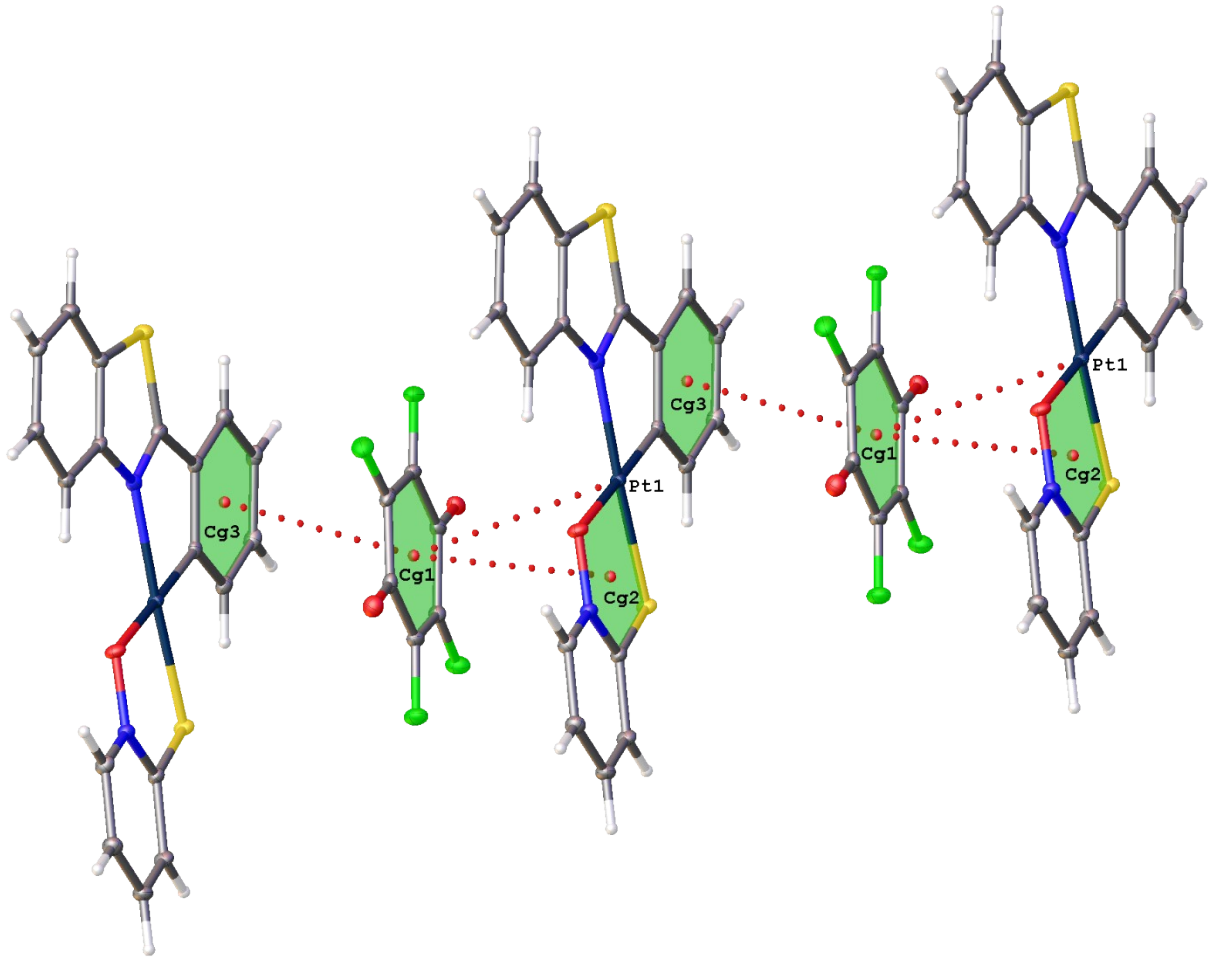


Figure S6. A fragment of crystal packing of **1**·QF ($\text{Cg}\cdots\text{Pt}$ and $\pi\cdots\pi$ interactions are given by dotted lines).

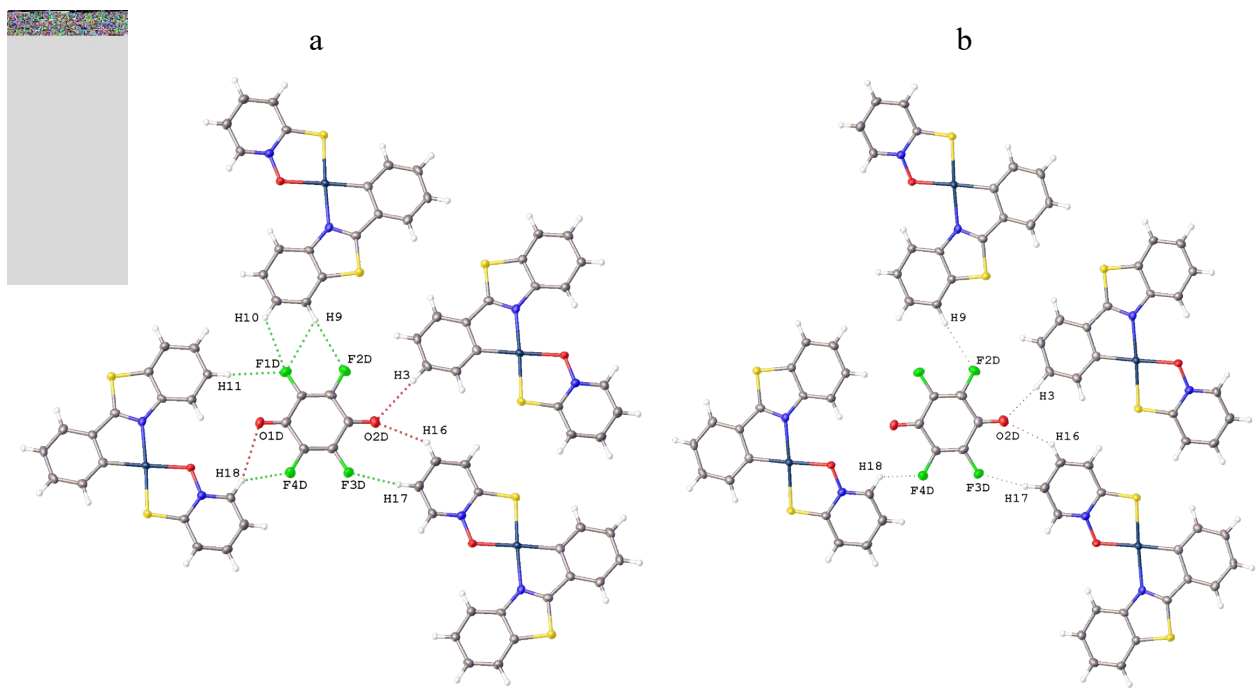


Figure S7. Fragments (a and b) of the crystal structure of **1**·QF with intermolecular HBs given by dotted lines.

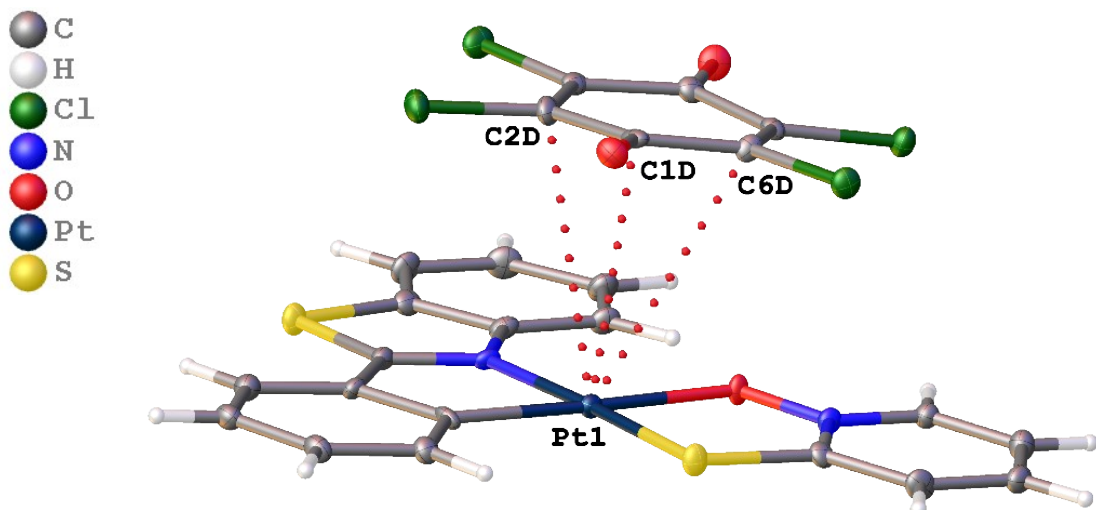


Figure S8. Molecular structure of **1**·QCl showing C···Pt contacts in dotted lines.

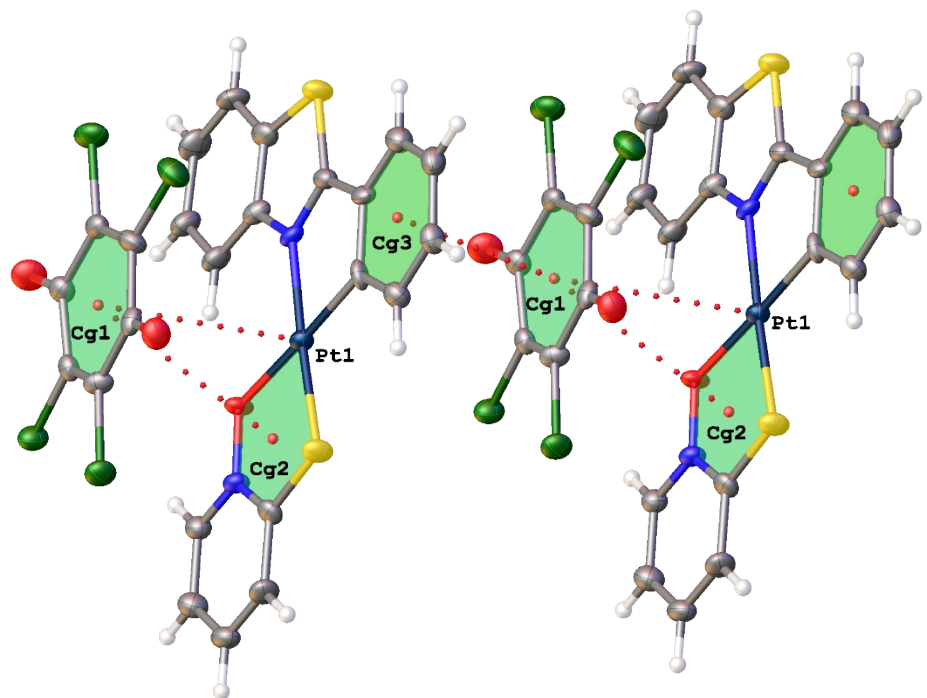


Figure S9. Fragment of crystal packing of **1·QCl** ($\text{Cg}\cdots\text{Pt}$ and $\pi\cdots\pi$ interactions are in dotted lines).

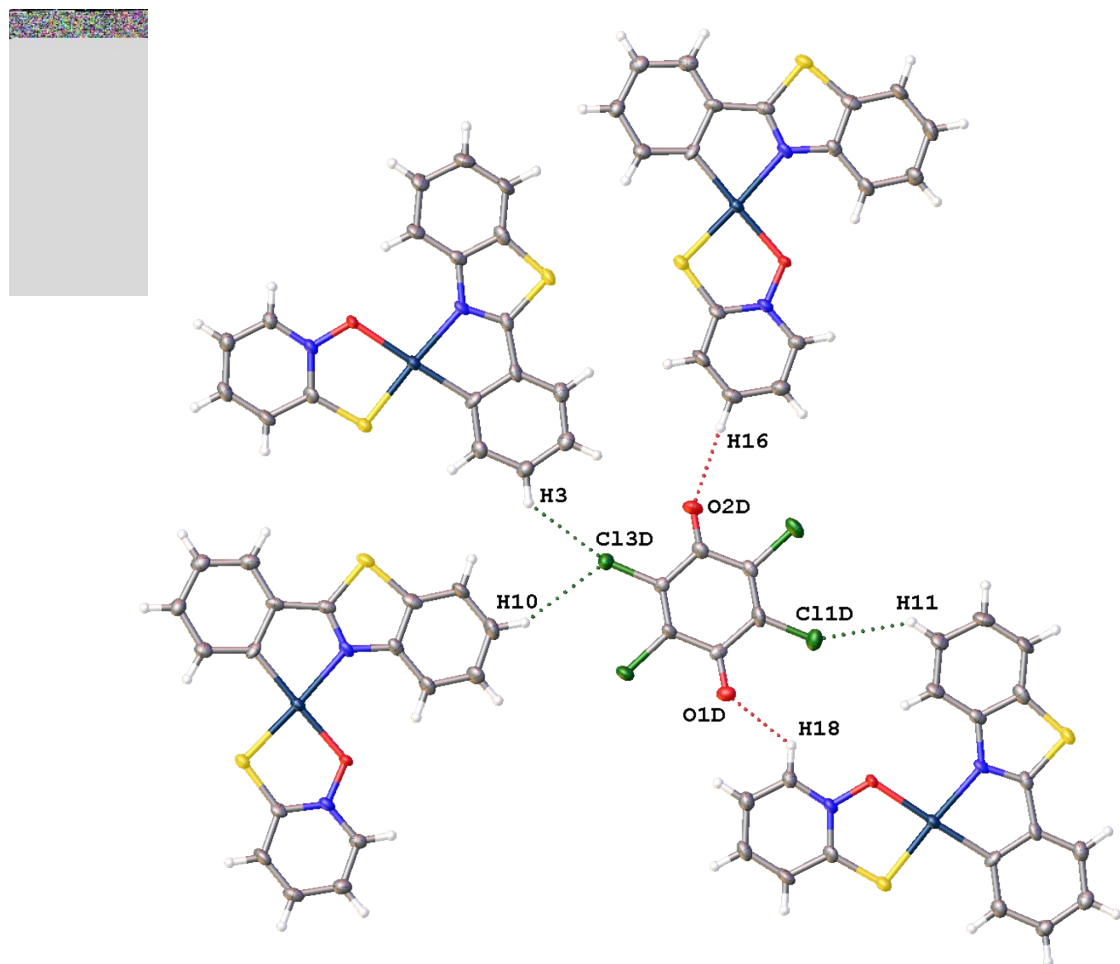


Figure S10. Fragment of the crystal structure of **1·QCl** showing intermolecular HBs (dotted lines).

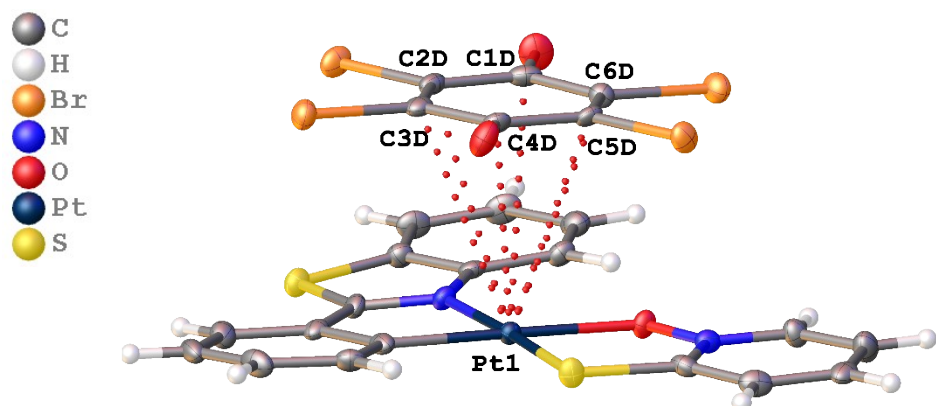


Figure S11. Molecular structure of **1·QBr** showing C···Pt contacts (dotted lines).

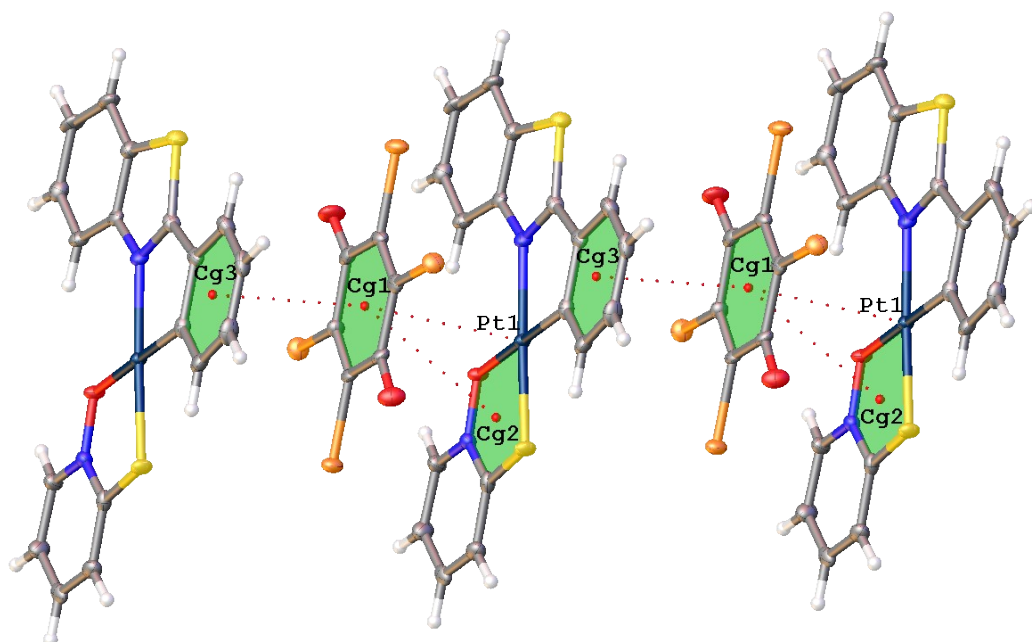


Figure S12. Fragment of crystal packing of **1·QBr** ($\text{Cg}\cdots\text{Pt}$ and $\pi\cdots\pi$ separations are in dotted lines).

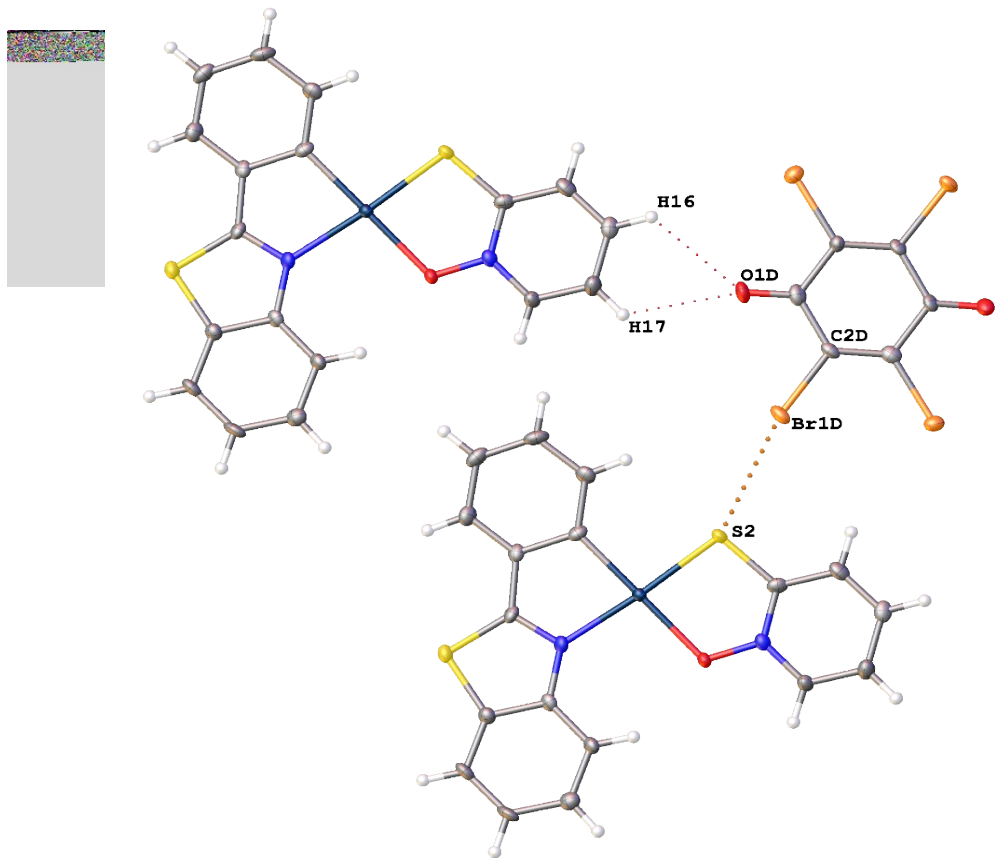


Figure S13. Fragment of the crystal structure of **1·QBr** showing intermolecular HBs (red dotted lines) and HaB (orange dotted line).

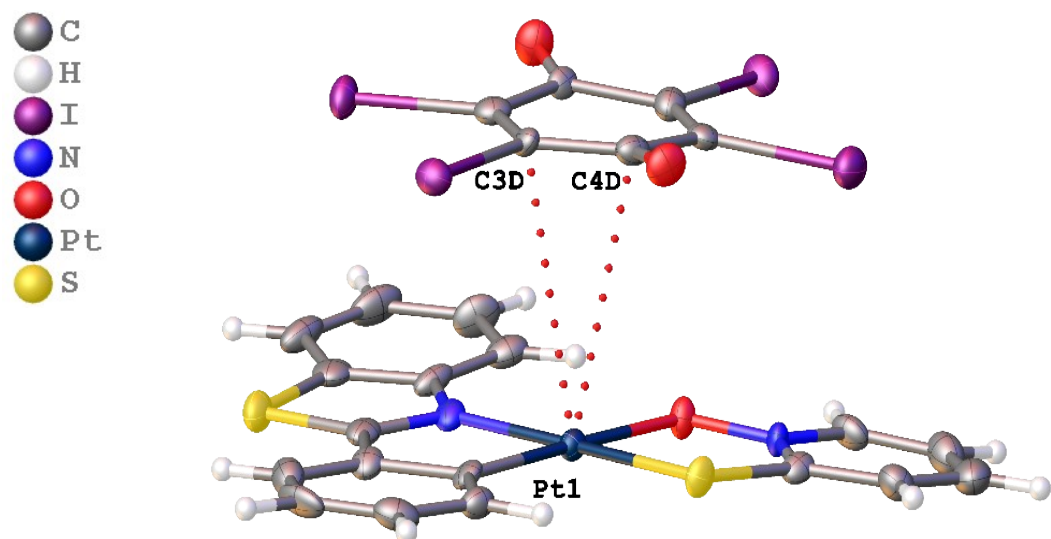


Figure S14. Molecular structure of **1·QI** with C···Pt contacts in dotted lines.

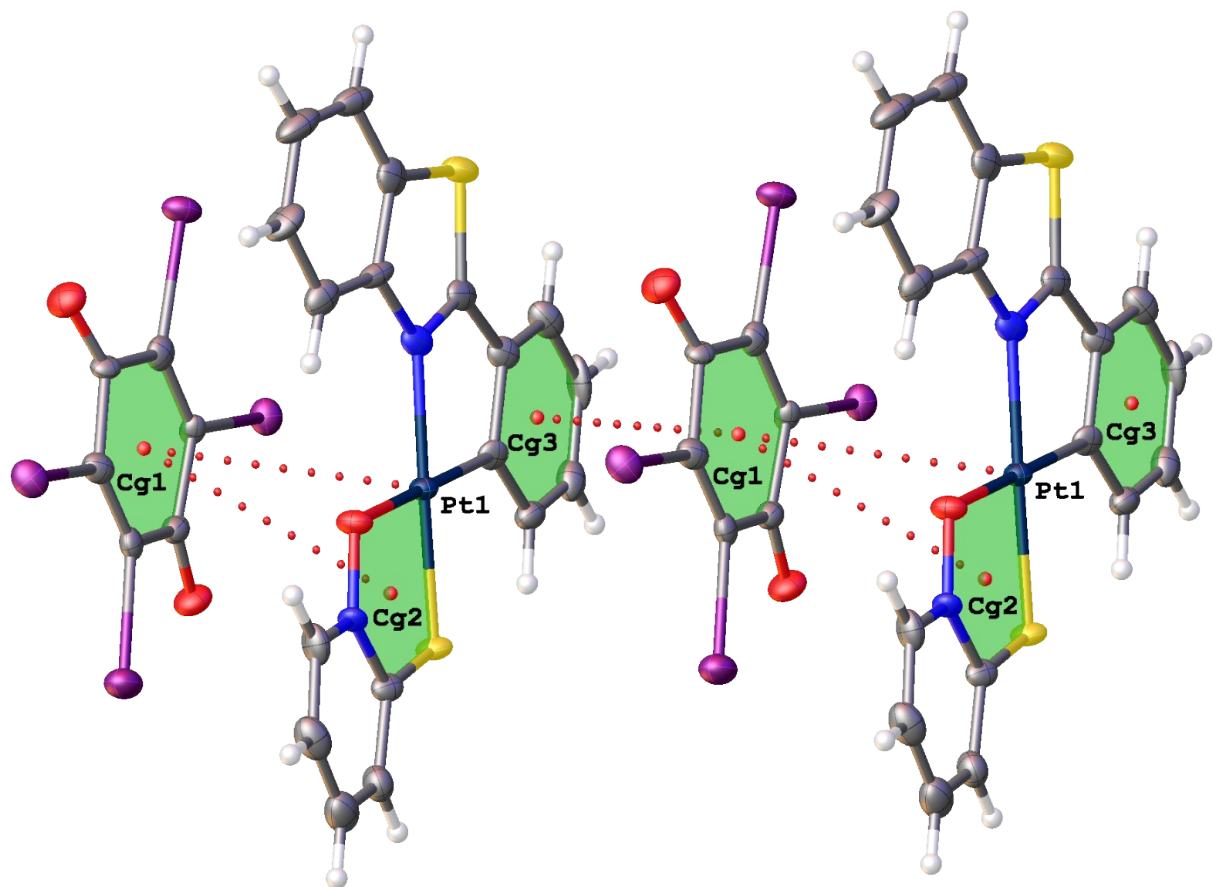


Figure S15. Fragment of crystal packing of **1·QI** ($\text{Cg}\cdots\text{Pt}$ and $\pi\cdots\pi$ interactions are dotted line).

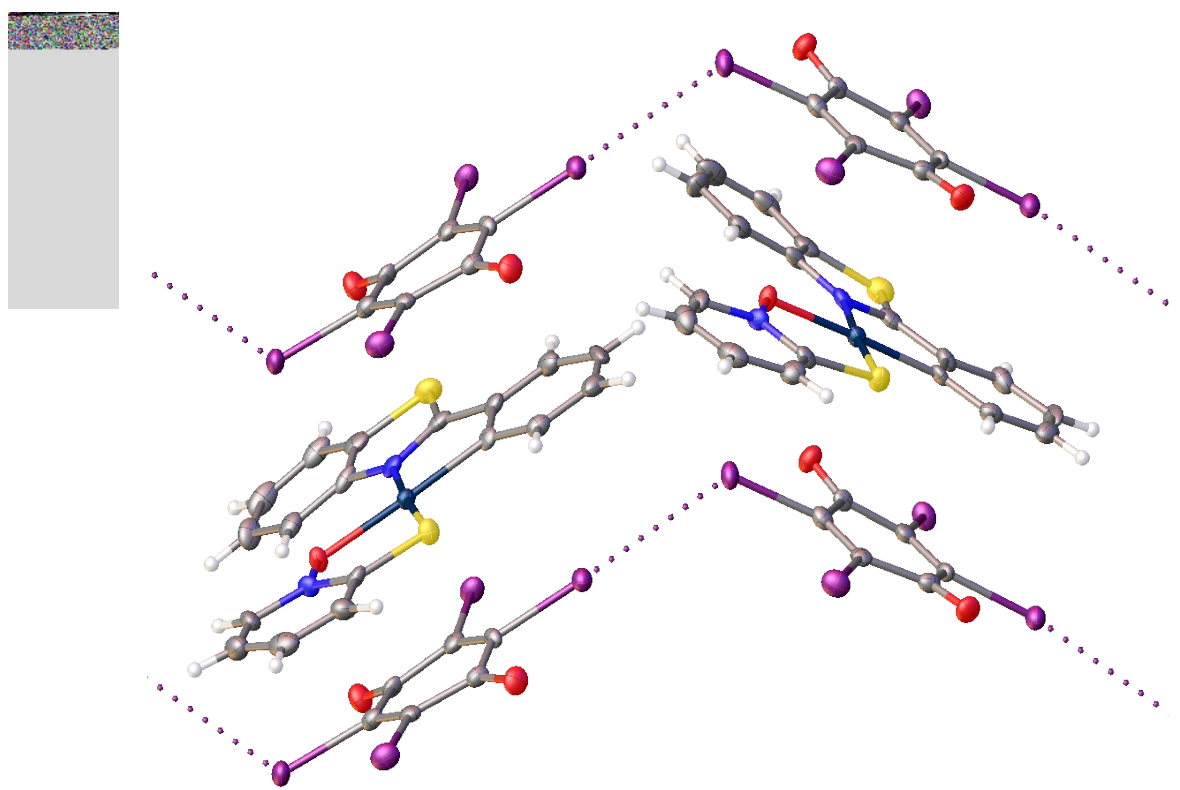


Figure S16. HaB between QI molecules in the structure of **1·QI**.

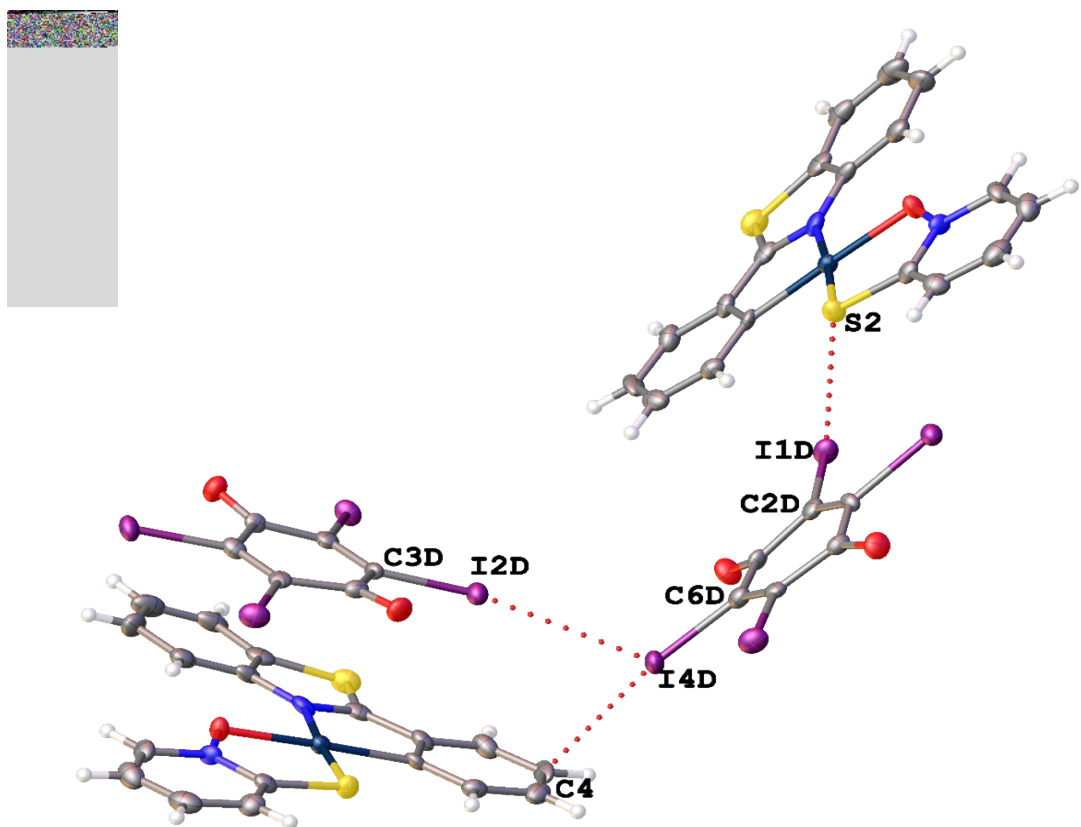


Figure S17. Fragment of the crystal structure of **1·QI**; HaBs are given in dotted lines.

S2. THERMOGRAVIMETRIC ANALYSIS

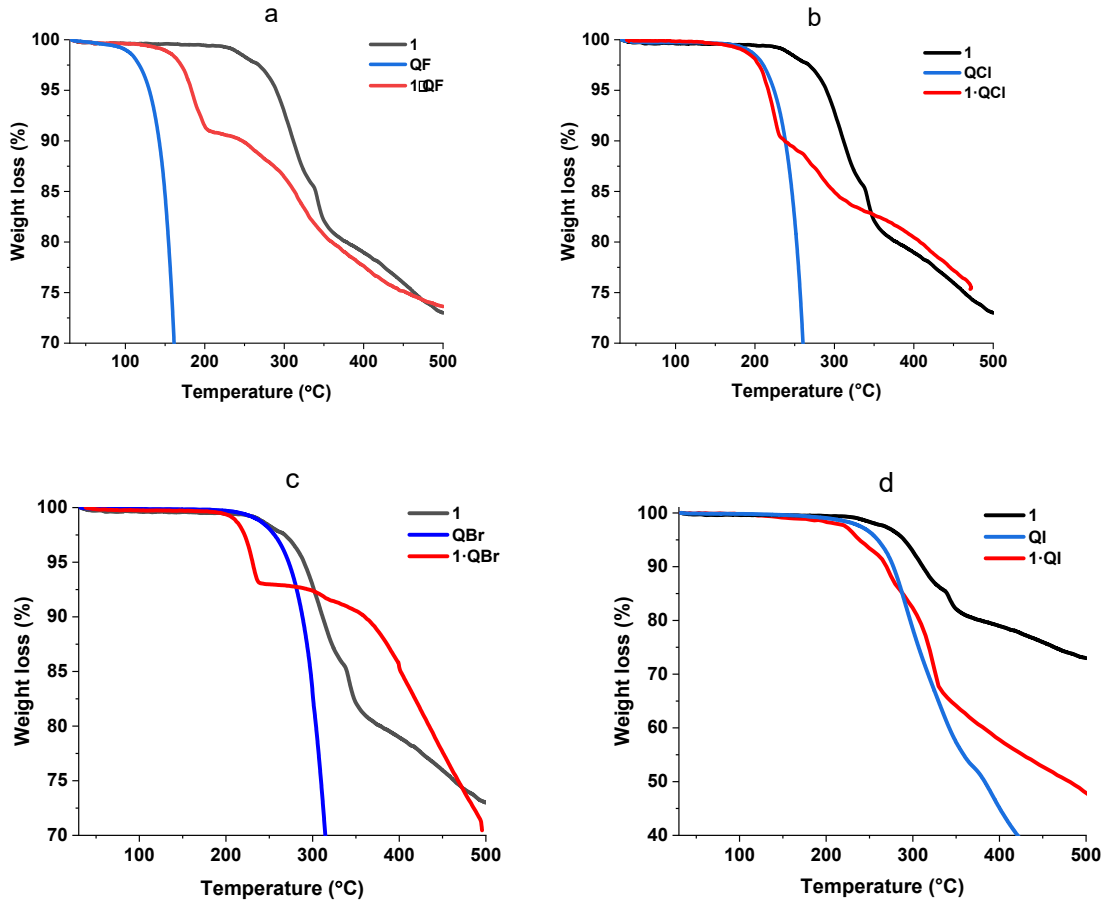


Figure S18. TGA curves of crystal samples of **1** (black), **QX** (blue) and **1·QX** (red).

Thermal properties. The thermal behavior of **1·QX** is different from that of **1**. On the thermogravimetric (TG) curves, for **1·QX**, the first mass-loss was observed at 166 °C (8% weight loss, **1·QF**), 204 °C (8% weight loss, **1·QCl**), 351 °C (8% weight loss, **1·QBr**), and 273 °C (29% weight loss, **1·QI**) (**Figure S18**). The parent complex **1** exhibits highest thermal stability among measured **1·QX** and it starts to decompose at 275 °C (8% weight loss).

S3. SOLID-STATE ^{195}Pt NMR SPECTRA

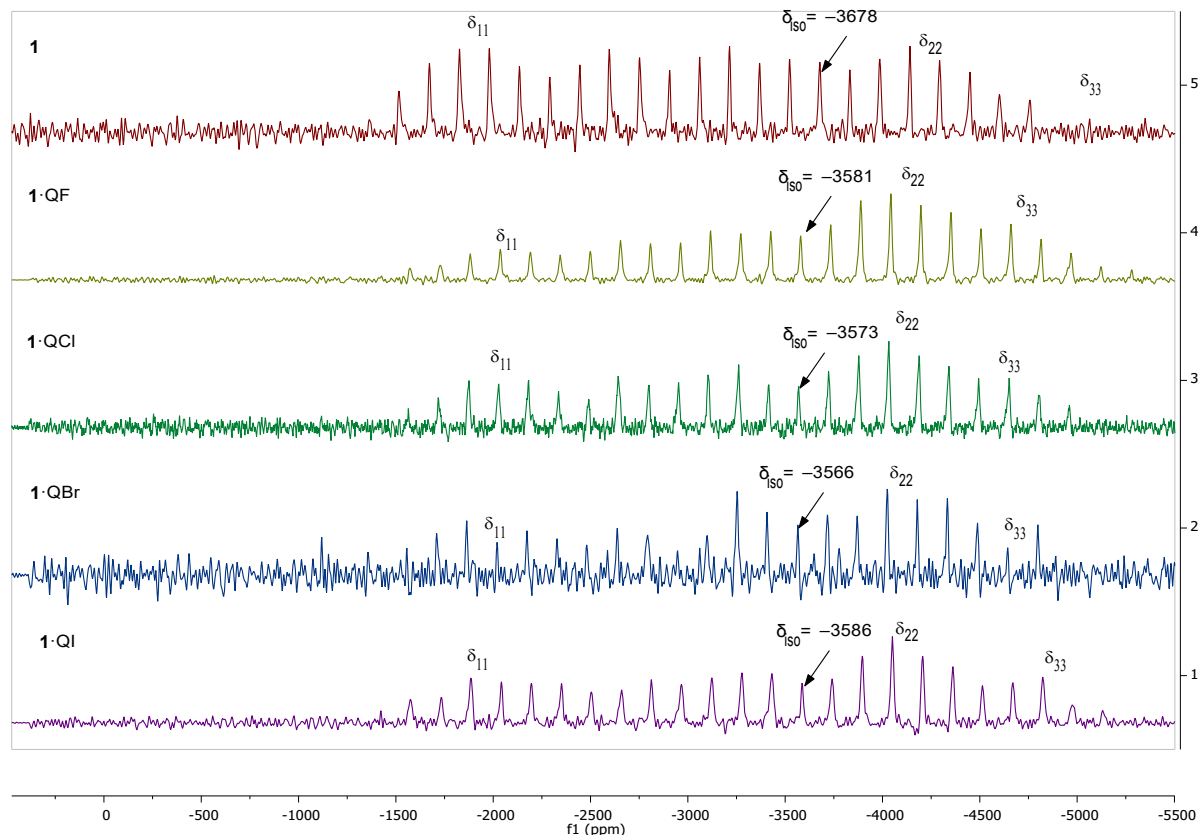


Figure S19. ^{195}Pt solid-state NMR overlayed spectra for **1**, **1·QF**, **1·QCl**, **1·QBr** and **1·QI** (MAS rotation frequency 13.3 kHz).

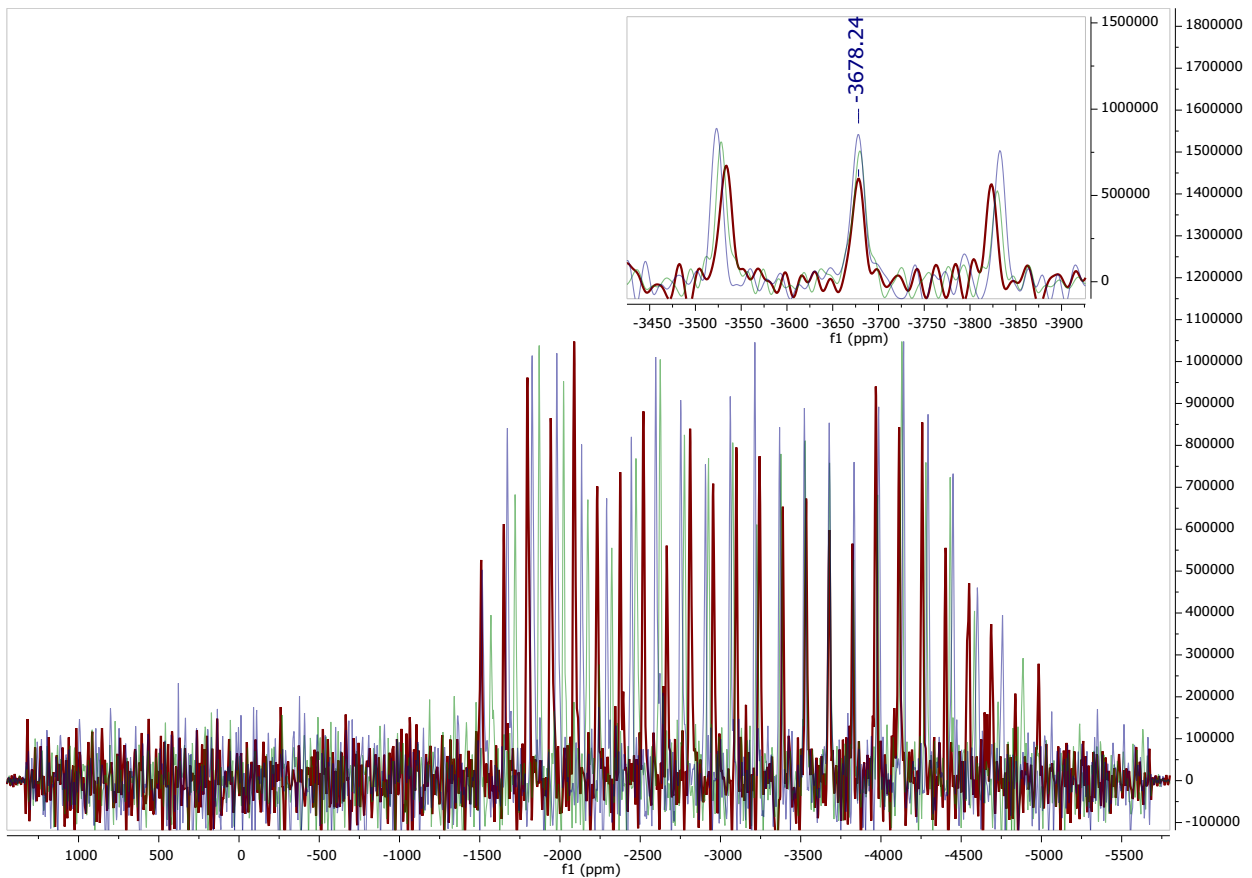


Figure S20. ¹⁹⁵Pt solid-state NMR overlayed spectra for **1** at 12.5 kHz (red) 13.0 kHz (green) and 13.3 kHz (blue) MAS rotation frequency (inset: enlarged part of spectra to determine δ_{iso}).

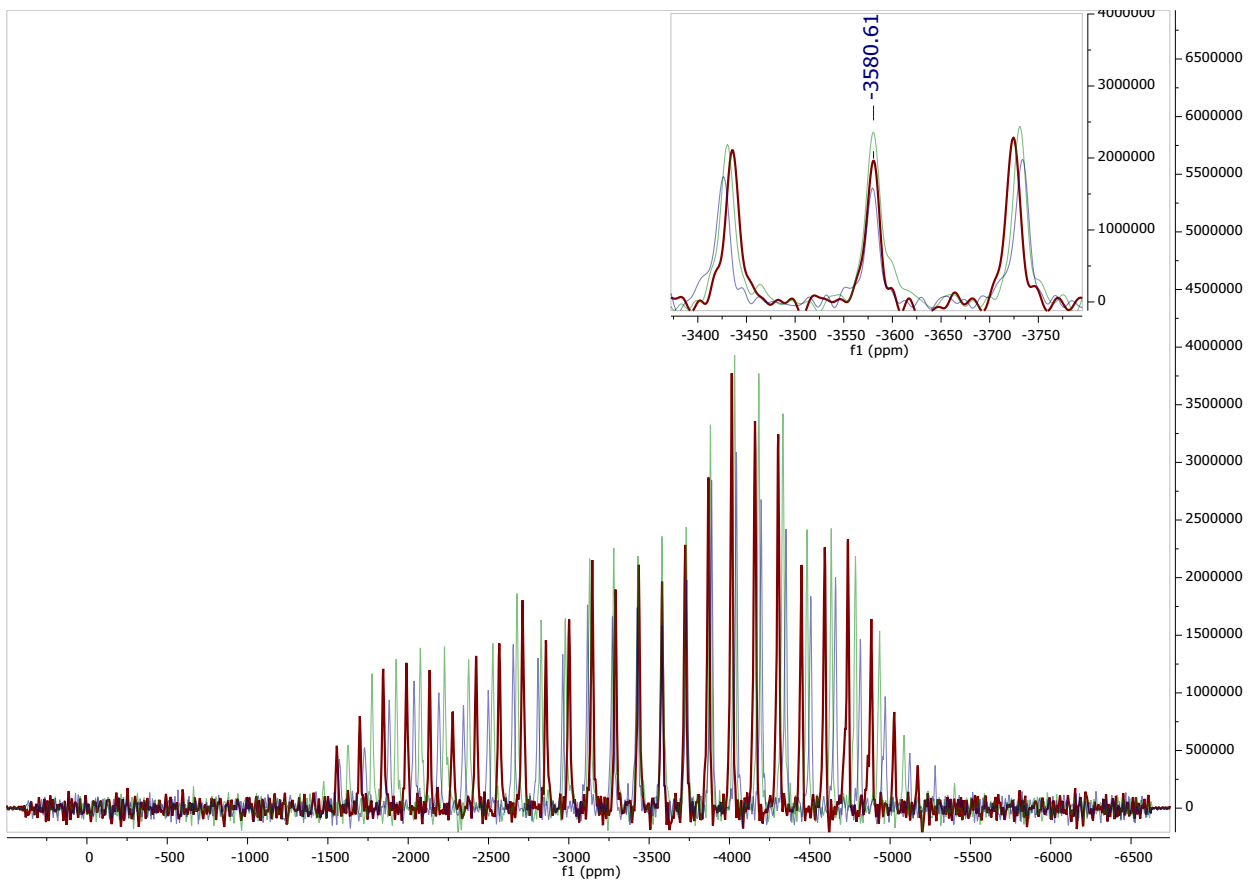


Figure S21. ¹⁹⁵Pt solid-state NMR overlayed spectra for **1**·QF at 12.5 kHz (red) 13.0 kHz (green) and 13.3 kHz (blue) MAS rotation frequency (inset: enlarged part of spectra to determine δ_{iso}).

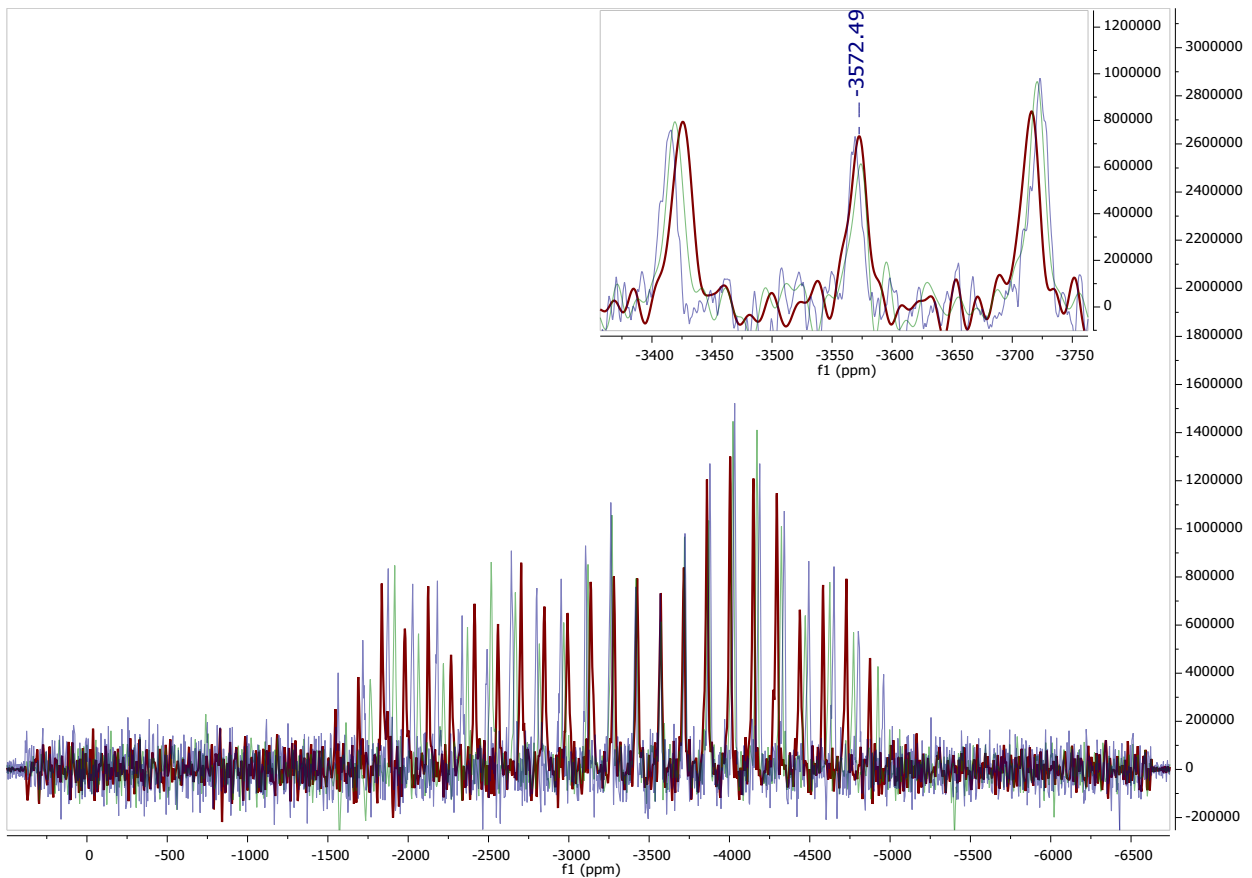


Figure S22. ¹⁹⁵Pt solid-state NMR overlayed spectra for **1·QCl** at 12.5 kHz (red) 13.0 kHz (green) and 13.3 kHz (blue) MAS rotation frequency (inset: enlarged part of spectra to determine δ_{iso}).

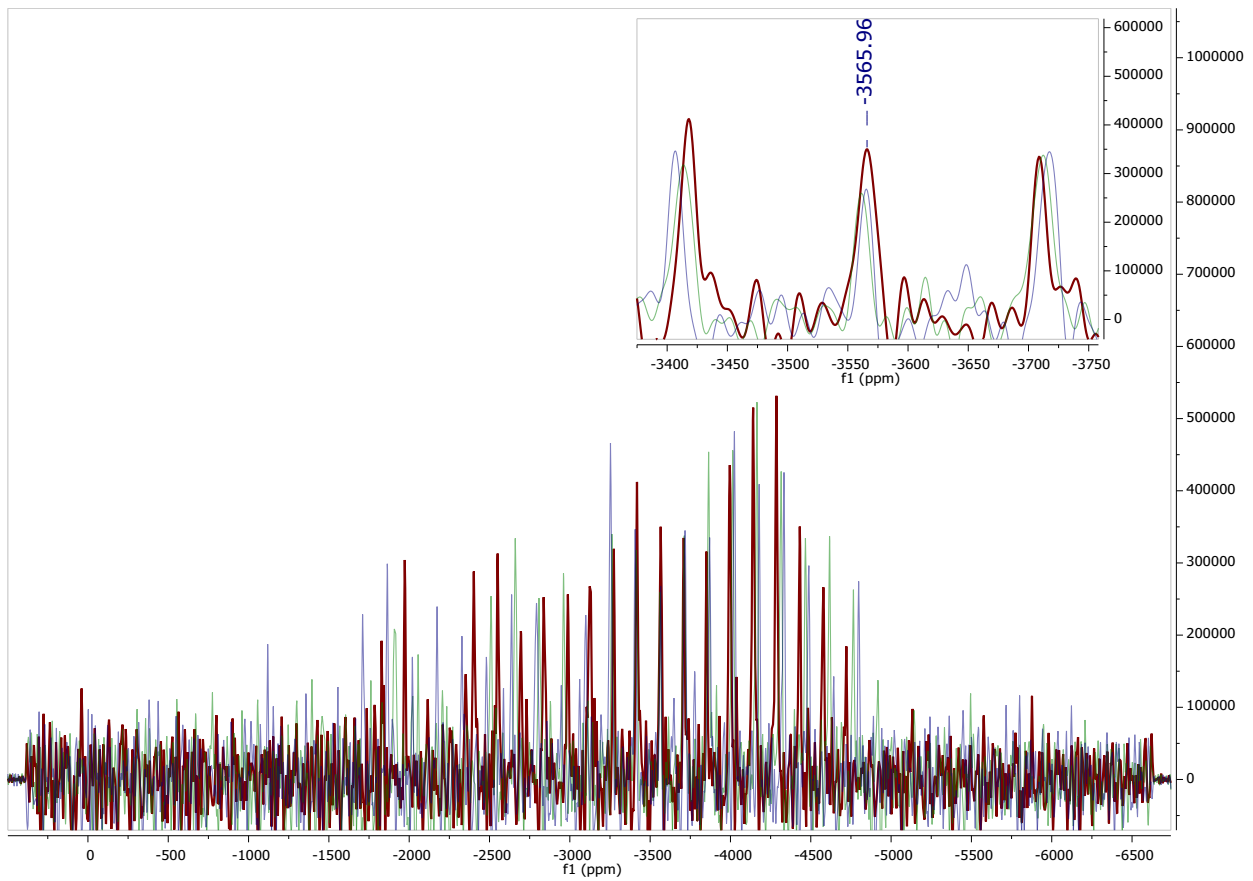


Figure S23. ¹⁹⁵Pt solid-state NMR overlayed spectra for **1·QBr** at 12.5 kHz (red) 13.0 kHz (green) and 13.3 kHz (blue) MAS rotation frequency (inset: enlarged part of spectra to determine δ_{iso}).

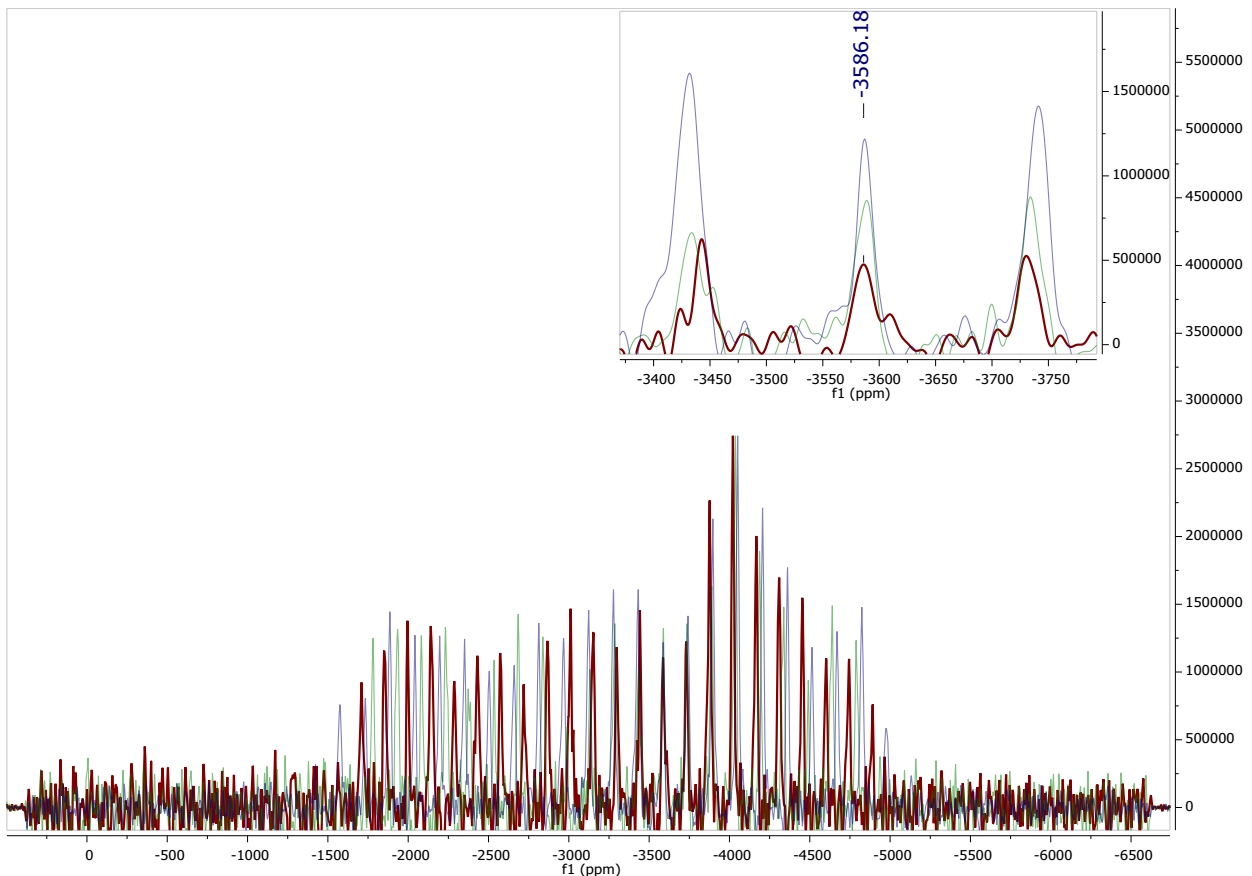


Figure S24. ^{195}Pt solid-state NMR overlayed spectra for **1·QI** at 12.5 kHz (red) 13.0 kHz (green) and 13.3 kHz (blue) MAS rotation frequency (inset: enlarged part of spectra to determine δ_{iso}).

Analysis of the ^{195}Pt MAS-NMR spectra, measured at different spinning rates (12.5, 13.0, and 13.3 kHz), allowed the assignment of the isotropic ^{195}Pt chemical shifts (δ_{iso}). We found that δ_{iso} in the cocrystals are low-field shifted and $\Delta\delta_{\text{iso}}$ is in the range 92–112 ppm (Table 2, Figures S19–24). To interpret the obtained NMR data, we performed theoretical calculations of the magnetic shielding tensor and magnetically induced currents for the bimolecular models [**1·QX**] and also for the parent complex **1** (Table S3). As a whole, the calculated isotropic shift correlates well with the experimentally observed one. However, we found a discrepancy of the δ_{iso} between the theoretical and experimental data (Table S3), most likely because all noncovalent interactions were not considered in the bimolecular model.

The disc-like shaped orientations of the calculated magnetic shielding tensors are nearly the same for all systems. The σ_{11} axis of the tensor is directed perpendicularly to the molecular plane, while the σ_{33} axis is oriented toward the C \cap N and N \cap O chelated rings (Figure S5). The directions of the σ_{11} and σ_{33} tensors are most susceptible to all structural changes accompanied the generation of the adducts.

Next, the skew parameter (κ) increases from -0.53 to -0.47 ongoing from **1**·QF to **1**·QI. The κ value for **1**·QI is practically the same as in the parent complex **1** (-0.48). According to refs¹⁻³, the changes in the κ values are associated with the deshielding effect oriented perpendicularly to the complex square-plane. The occurrence of intermolecular contacts between **1** and QX is also affected by the local environment around the Pt-atom, as reflected by a significant change in Ω on pairing of the coformers (3727 ppm for **1**; 2620 **1**·QF; 2604 **1**·QCl; 2644 **1**·QBr; 2935 **1**·QI). Usually, strengthening of noncovalent interactions leads to a higher polarization of the electronic density of the system and this effect is accompanied by appropriate changes in density of the magnetically induced current (MIC) within the overall system.^{4, 5} Hence, visualization of MIC and quantitative estimate of the density along chemical bonds under study are useful parameters to understand reasons of the observed chemical shift. The analysis of MIC for the Pt–C, Pt–N, Pt–S, and N–C (in *pbt*-ligand) bonds revealed that the noncovalent interaction of **1** with any one of QX leads to an increase in diatropic and paratropic currents by 0.45–0.12 nT/A within the chelated rings. This effect increases in the series from [**1**·QI] to [**1**·QF] (**Table S3**). Such trend in the MIC density values is probably due to the polarization of electronic density from **1** toward QX.

Thus, we can conclude that the induction of ring currents in the QX molecule affects the MIC ring currents of **1**, resulting in changes in the tensor components in the adducts. This is attributed to the formation of the [**1**·QX] adducts.

Table S3. Calculated Solid-State ^{195}Pt NMR Parameters of **1** and **1**·QX (X = F, Cl, Br, I)

	δ_{11} , ppm	δ_{22} , ppm	δ_{33} , ppm	δ_{iso} , ppm	Ω , ppm	κ
1	-3387	-4500	-5028	-4305	1641	-0.36
1 ·QF	-2673	-4957	-5053	-4228	2380	-0.92
1 ·QCl	-2496	-4859	-5238	-4198	2742	-0.72
1 ·QBr	-2502	-4871	-5247	-4207	2745	-0.73
1 ·QI	-2583	-4992	-5207	-4261	2624	-0.84

S4. CALCULATION DETAILS

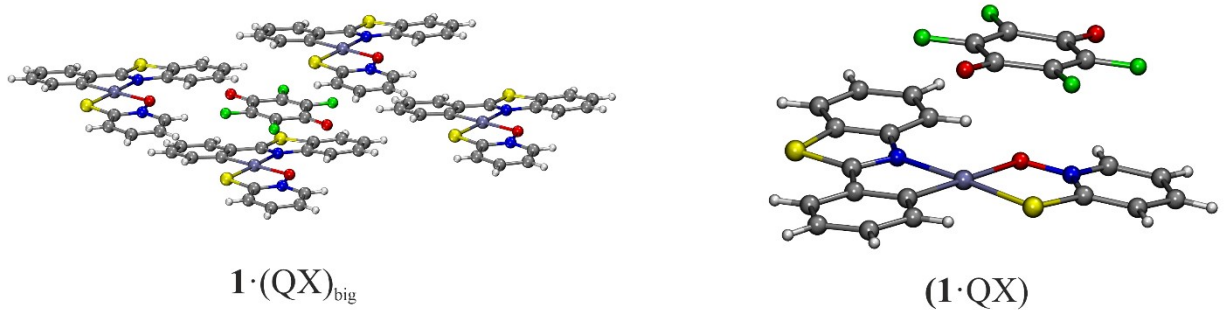


Figure S25. Clusters used in calculations.

Table S4. Electron density (ρ_b), its Laplacian ($\nabla^2\rho_b$), potential and kinetic energy densities (V_b and G_b), second eigenvalue of the Hessian matrix (λ_2), electron localization function at BCPs (in a.u.), and IBSI.

Contact	Clusters	ρ_b	$\nabla^2\rho_b$	V_b	G_b	H_b	λ_2	ELF
C1D···Pt	[1·QF]	0.0109	0.0279	-0.0055	0.0062	-0.0007	-0.0016	0.058
C1D···Pt	(1·QF)	0.0106	0.0298	-0.0052	0.0063	0.0011	-0.0029	0.051
C1D···Pt	(1·QF) _{big}	0.0108	0.0275	-0.0054	0.0062	0.0007	-0.0018	0.0567
C3D···Pt	[1·QCl]	0.0084	0.0217	-0.0040	0.0047	-0.0007	-0.0020	0.042
C3D···Pt	(1·QCl)	0.0076	0.0206	-0.0034	0.0043	-0.0009	-0.0015	0.037
C3D···Pt	(1·QCl) _{big}	0.0086	0.0214	-0.0038	0.0042	-0.0006	-0.0022	0.044
C3D···Pt	[1·QBr]	0.0070	0.0187	-0.0032	0.0039	-0.0007	-0.0011	0.033
C3D···Pt	(1·QBr)	0.0066	0.0158	-0.0031	0.0035	-0.0004	-0.0017	0.035
C3D···Pt	(1·QBr) _{big}	0.0071	0.0188	-0.0030	0.0037	-0.0006	-0.0009	0.030
C3D···Pt1	[1·QI]	0.0065	0.0175	-0.0175	0.0037	0.0007	-0.0009	0.030
C3D···Pt	(1·QI)	0.0059	0.0154	-0.0026	0.0032	0.0006	-0.0014	0.0288

C3D···Pt	(1·QI) _{big}	0.0060	0.0156	-0.0027	0.0030	0.0005	-0.0014	0.0287
----------	-----------------------	--------	--------	---------	--------	--------	---------	--------

Table S5. Contact distance (d) in Å, ratio between the distance and Alvarez Σ_{vdW} (R), electron density (ρ_b), its Laplacian ($\nabla^2 \rho_b$), potential and kinetic energy densities (V_b and G_b), second eigenvalue of the Hessian matrix (λ_2), elliptical bond index (ε) (in a.u.), electron localization function at BCPs, and IBSI and dg_{pair} at the PBE0-D3BJ/ZORA-def2-TZVP and PBE-D3BJ/ZORA-def2-TZVP (in parentheses for [1·QF]) levels of theory.

[1·QF]												
Contact	d	R	ρ_b	$\nabla^2 \rho_b$	V_b	G_b	H(r)	ε	λ_2	ELF	IBSI	dg_{pair}
C6D···Pt1	3.369	0.91	0.0115 (0.0115)	0.0286 (0.0270)	-0.0058 (-0.0053)	0.0065 (0.0061)	0.0007 (0.0007)	4.5504 (2.0725)	-0.0014 (-0.0022)	0.0628 (0.0705)	0.0140	0.0646
C1D···Pt1	3.323	0.82									0.0150	0.0672
C2D···Pt1	3.632	0.89									0.0081	0.0433
C3D···Pt1	3.965	0.98									0.0041	0.0263
C4D···Pt1	4.025	0.99									0.0039	0.0255
C5D···Pt1	3.739	0.92									0.0068	0.0385
C4D···O1	3.075	0.91	0.0071 (0.070)	0.0275 (0.0265)	-0.0040 (-0.0039)	0.0054 (0.0052)	0.0014 (0.0014)	0.3732 (0.2408)	-0.0029 (-0.0030)	0.0185 (0.0191)	0.0092	0.0352
C18···O2D	3.161	0.97	0.0057 (0.0050)	0.0230 (0.0197)	-0.0030 (-0.0025)	0.0044 (0.0037)	0.0014 (0.0012)	0.4963 (0.6043)	-0.0025 (-0.021)	0.0139 (0.0129)	0.0066	0.0269
C12···F2D	3.289	1.02	0.0041 (0.0049)	0.0166 (0.0190)	-0.0021 (-0.0025)	0.0031 (0.0036)	0.0010 (0.0011)	0.5716 (0.2386)	-0.0017 (-0.0026)	0.0095 (0.0123)	0.0042	0.0183
C13···F1D	3.204	0.99	0.0048 (0.0050)	0.0223 (0.0240)	-0.0027 (-0.0029)	0.0042 (0.0044)	0.0014 (0.0016)	3.9902 (7.579)	-0.0005 (-0.004)	0.0085 (0.0092)	0.0051	0.0212
C14···F3D	3.282	1.02									0.0040	0.0173
N1···C2D	3.255	0.95									0.0069	0.0296

[1·QCl]												
Contact	d	R	ρ_b	$\nabla^2 \rho_b$	V_b	G_b	H(r)	ε	λ_2	ELF	IBSI	dg_{pair}
C3D···Pt1	3.562	0.88	0.0084	0.0217	-0.0040	0.0047	0.0007	1.3753	-0.0020	0.0423	0.0096	0.0494
C1D···Pt1	3.797	0.94									0.0058	0.0339
C2D···Pt1	3.651	0.90									0.0080	0.0432
C4D···Pt1	3.612	0.89									0.0079	0.0420
C5D···Pt1	3.837	0.95									0.0051	0.0308
C6D···Pt1	3.914	0.96									0.0048	0.0301
C12···O2D	3.530	1.08	0.0027	0.0106	-0.0012	0.0019	0.0007	0.5485	-0.0010	0.0064	0.0030	0.0149
C18···Cl3D	3.480	0.97	0.0058	0.0204	-0.0028	0.0039	0.0012	1.5291	-0.0015	0.0185	0.0062	0.0307

C6···Cl1D	3.658	1.02	0.0049	0.0177	-0.0022	0.0033	0.0011	2.4562	-0.0006	0.0144	0.0046	0.0250
C13···Cl3D	3.606	1.01									0.0062	0.0307
N1···Cl2D	3.491	1.00	0.0054	0.0220	-0.0027	0.0041	0.0014	0.8435	-0.0016	0.0135	0.0052	0.0255
C7···C2D	3.583	0.99									0.0051	0.0268
S2···C6D	3.515	0.96	0.0067	0.0201	-0.0030	0.0040	0.0010	0.3813	-0.0021	0.0274	0.0084	0.0421

[1·QBr]

Contact	d	R	ρ_b	$\nabla^2 \rho_b$	V_b	G_b	H(r)	ε	λ_2	ELF	IBSI	dg_{pair}
C1D···Pt1	3.652	0.90	0.0079	0.0206	-0.0037	0.0044	0.0007	1.4355	-0.0018	0.0397	0.0073	0.0396
C2D···Pt1	3.600	0.87									0.0088	0.0461
C3D···Pt1	3.663	0.90									0.0078	0.0423
C4D···Pt1	3.785	0.93									0.0060	0.0344
C5D···Pt1	3.937	0.97									0.0046	0.0289
C6D···Pt1	3.885	0.96									0.0046	0.0286
C2···O2D	3.697	1.13	0.0023	0.0084	-0.0009	0.0015	0.0006	0.8781	-0.0004	0.0056	0.0021	0.0116
C12···O1D	3.567	1.09	0.0026	0.0102	-0.0011	0.0018	0.0007	0.7196	-0.0009	0.0059	0.0027	0.0142
C18···Br4D	3.586	0.99	0.0060	0.0189	-0.0028	0.0038	0.0009	0.9221	-0.0019	0.0226	0.0066	0.0345
C1···Br2D	3.713	1.02	0.0052	0.0173	-0.0024	0.0033	0.0010	8.6088	-0.0003	0.0175	0.0054	0.0304
C13···Br1D	3.646	1.00									0.0058	0.0314
C7···Br1D	3.742	1.03									0.0049	0.0276
C6···Br2D	3.720	1.02									0.0051	0.0285
N1···Br1D	3.612	1.03	0.0054	0.0204	-0.0026	0.0039	0.0012	1.6101	-0.0010	0.0147	0.0055	0.0292
N2···Br4D	3.599	1.02									0.0050	0.0263
S2···C4D	3.684	1.01	0.0067	0.0200	-0.0030	0.0040	0.0010	0.5042	-0.0020	0.0282	0.0058	0.0318
S2···Br3D	3.884	1.04									0.0063	0.0386

[1·QI]

Contact	d	R	ρ_b	$\nabla^2 \rho_b$	V_b	G_b	H(r)	ε	λ_2	ELF	IBSI	dg_{pair}
C3D···Pt1	3.764	0.93	0.0061	0.0167	-0.0028	0.0035	0.0007	8.7805	-0.0003	0.0271	0.0061	0.0348
C5D···Pt1	3.703	0.91	0.0065	0.0175	0.0175	0.0037	0.0007	2.3199	-0.0009	0.0299	0.0071	0.0369
C1D···Pt1	3.862	0.95									0.0046	0.0281
C2D···Pt1	3.879	0.96									0.0048	0.0291
C4D···Pt1	3.636	0.90									0.0081	0.0433

C6D···Pt1	3.794	0.93									0.0057	0.0334
C12···O1D	3.279	1.00	0.0048	0.0184	-0.0023	0.0034	0.0012	0.6982	-0.0017	0.0125	0.0052	0.026
C13···O1D	3.445	1.05									0.0037	0.0176
C2···I2D	3.851	1.01	0.0056	0.0158	-0.0024	0.0032	0.0008	2.2043	-0.0009	0.0247	0.0058	0.0351
C14···I3D	3.694	0.97	0.0066	0.0187	-0.0031	0.0039	0.0008	0.6408	-0.0019	0.0284	0.0078	0.0435
C18···I4D	3.898	1.02	0.0046	0.0136	-0.0020	0.0027	0.0007	0.8181	-0.0014	0.0185	0.0053	0.0327
C3···I2D	3.916	1.03									0.0051	0.0319
C7···I1D	3.839	1.01									0.0057	0.0343
C15···I3D	3.902	1.02									0.0050	0.0307
S1···I1D	3.934	1.00	0.0065	0.0177	-0.0027	0.0036	0.0009	0.4333	-0.0025	0.0327	0.0079	0.0495
S2···I3D	4.098	1.04									0.0384	0.0056
H12···I4D	3.688	1.14	0.0026	0.0082	-0.0011	0.0016	0.0005	2.4849	-0.0004	0.0076	0.0023	0.0102

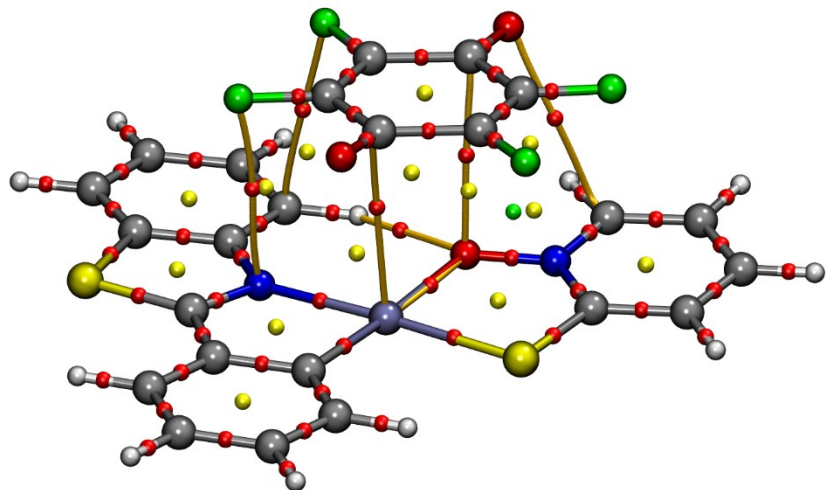


Figure S26. QTAIM distribution of bond, ring, and cage critical points (red, yellow, and green spheres, respectively) and bond paths for **[1·QF]**.

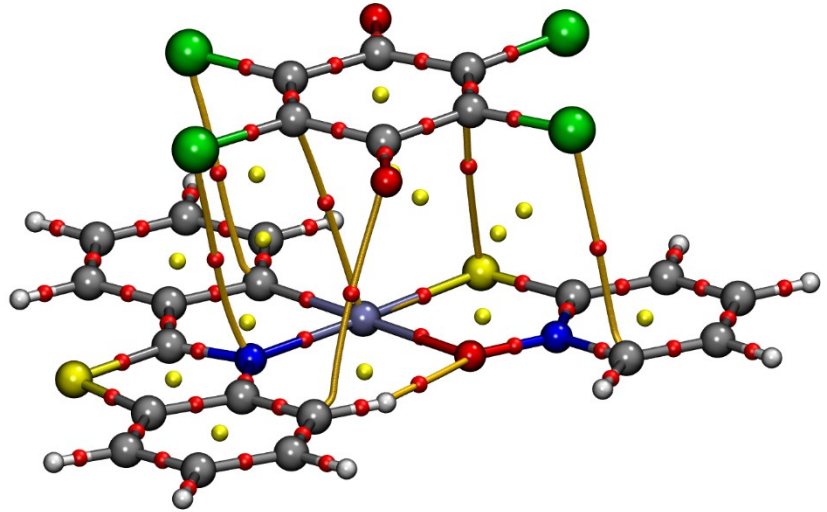


Figure S27. QTAIM distribution of bond, ring, and cage critical points (red, yellow, and green spheres, respectively) and bond paths for $[1 \cdot \text{QCl}]$.

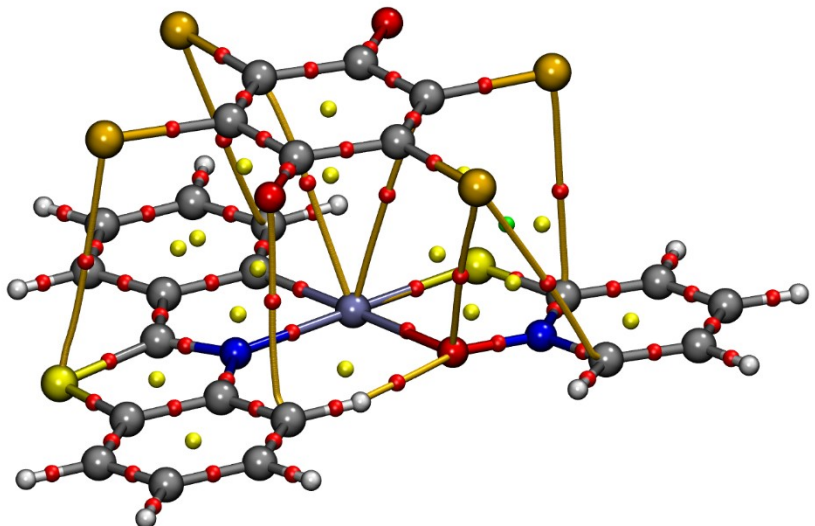


Figure S28. QTAIM distribution of bond, ring, and cage critical points (red, yellow, and green spheres, respectively) and bond paths for $[1 \cdot \text{QBr}]$.

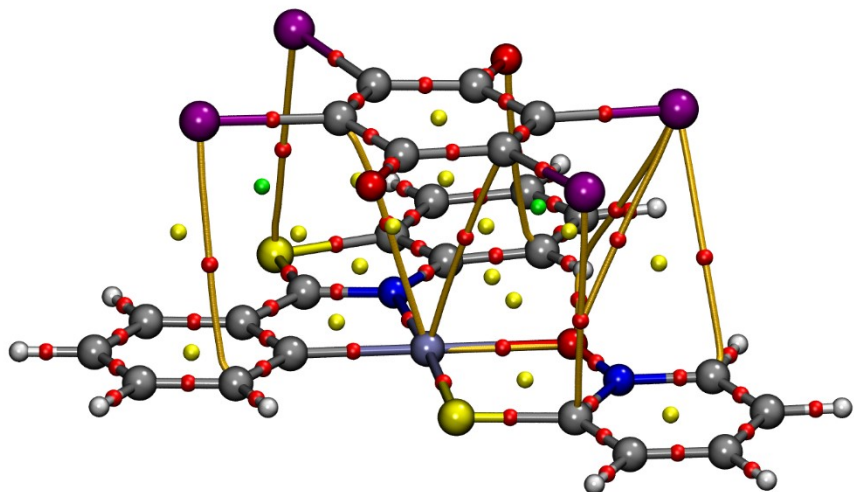


Figure S29. QTAIM distribution of bond, ring, and cage critical points (red, yellow, and green spheres, respectively) and bond paths for $[1\cdot\text{QI}]$.

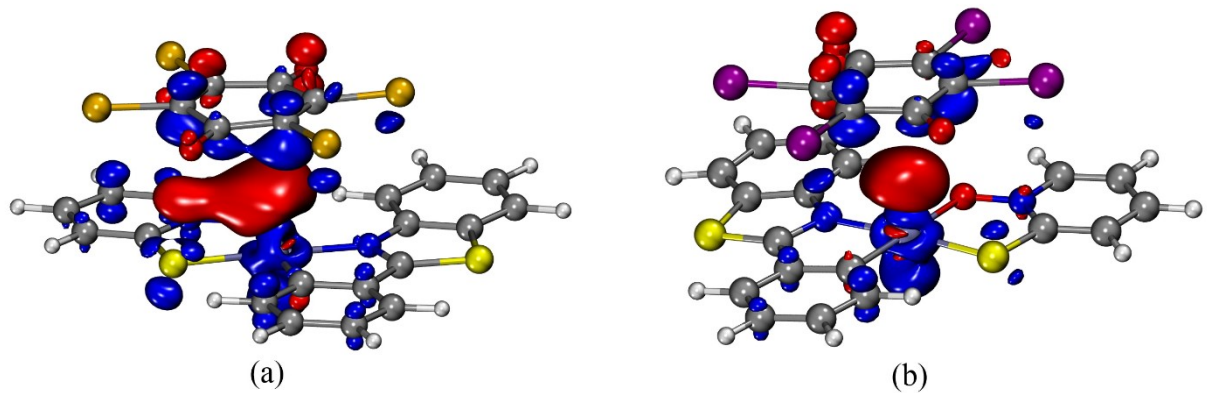


Figure S30. ETS-NOCV deformation densities for (a) $[1\cdot\text{QBr}]$ and (b) $[1\cdot\text{QI}]$ (isovalue 0.0005 and 0.005 a.u. , electrons transfer occurs from the decreased electron density regions (blue) to the increased electron density regions (red).

Geometry optimization

Analysis of the X-ray diffraction data shows that adducts **1·QX** are arranged in stacks, where the quinone molecule interacts with the Pt complexes. To exclude the effect of crystal packing on the interactions between **1** and a quinone, the full geometry optimization of two cluster models of the cocrystals **1·QX** was carried out, *i.e.* bimolecular and trimolecular clusters, $[1\cdot\text{QX}]$ and $[\text{QX } 1\cdot\text{QX}]$, respectively (**Figure S31**).

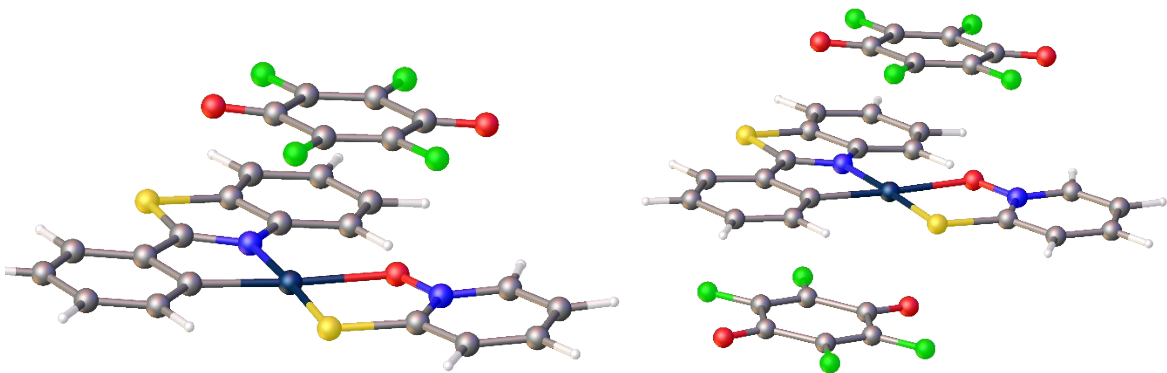


Figure S31. Schematic representation of bimolecular (*left*) and trimolecular (*right*) model clusters used for the calculations.

To distinguish quinone molecules from each other depending on the position relative to the complex, we introduced the designations QX^{A} and QX^{B} (see **Figure S32**).

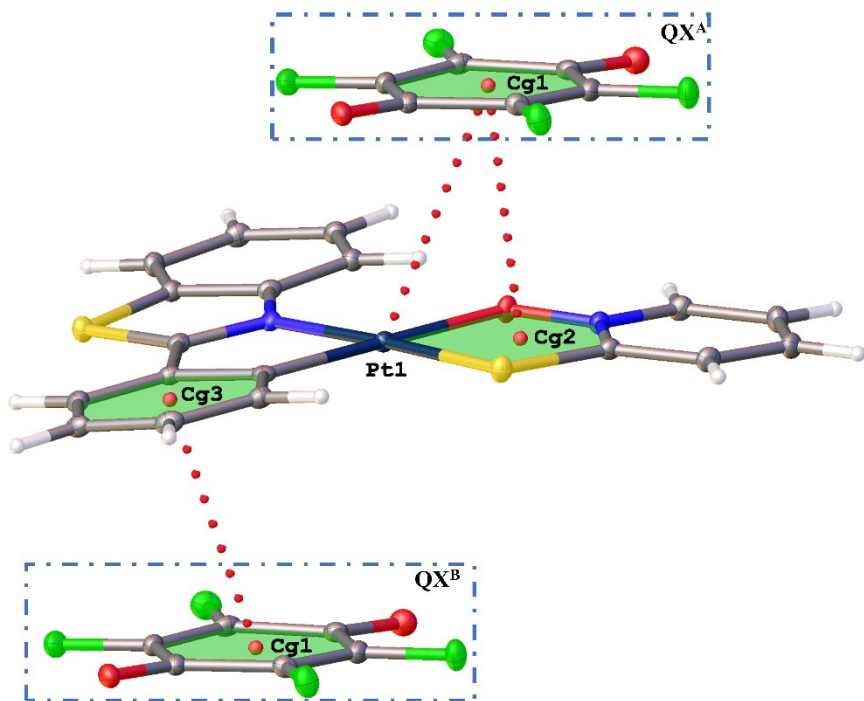


Figure S32. Schematic representation of QX^{A} and QX^{B} .

Comparison of the structural parameters of the X-ray and optimized structures indicates that the optimized geometries for **1** and QX^{A} of the bimolecular cluster models do not deviate significantly from the experimental structures (**Table S6**, **Figure S32**). At the same time, the optimization of trimolecular cluster resulted in the notable structural changes, *i.e.*, the QX^{B} molecule is strongly shifted relative to the X-ray structure (**Table S6**, **Figure S32**). Thus, in the further theoretical studies, the bimolecular model was used.

Table S6. Parameters of QX shifts.

Entry	<i>r</i> , Å		<i>α</i> , °	
	QX ^A	QX ^B	QX ^A	QX ^B
[QF ^A · 1 ·QF ^B] _{XRD}	1.578	2.972	25.7	56.0
[1 ·QF ^A]	0.920	—	15.7	—
[QF ^A · 1 ·QF ^B]	0.966	1.323	16.5	23.5
[QCl ^A · 1 ·QCl ^B] _{XRD}	1.222	2.811	18.0	38.3
[1 ·QCl ^A]	0.461	—	7.7	—
[QCl ^A · 1 ·QCl ^B]	0.468	0.094	7.8	1.6
[QBr ^A · 1 ·QBr ^B] _{XRD}	0.342	3.139	5.7	41.2
[1 ·QBr ^A]	0.463	—	7.8	—
[QBr ^A · 1 ·QBr ^B]	0.457	0.579	7.6	9.6
[QI ^A · 1 ·QI ^B] _{XRD}	1.566	2.623	23.5	36
[1 ·QI ^A]	1.226	—	20.5	—
[QI ^A · 1 ·QI ^B]	0.460	0.433	7.6	7.1

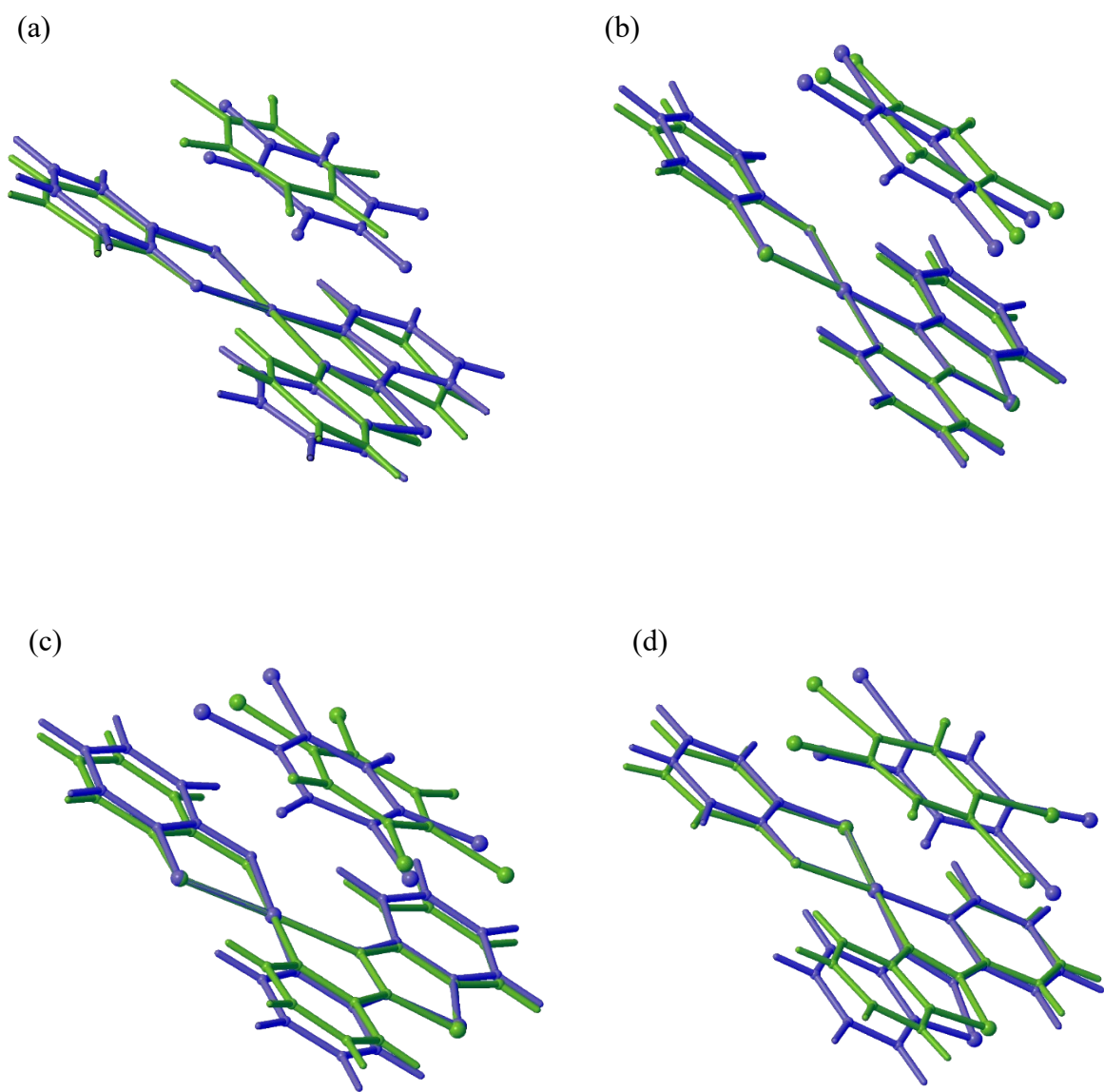


Figure S33. Overlayed images of **1**·QF (a) **1**·QCl (b), **1**·QBr (c) and **1**·QI (d) in X-ray (green) and optimized bimolecular (blue) geometries.

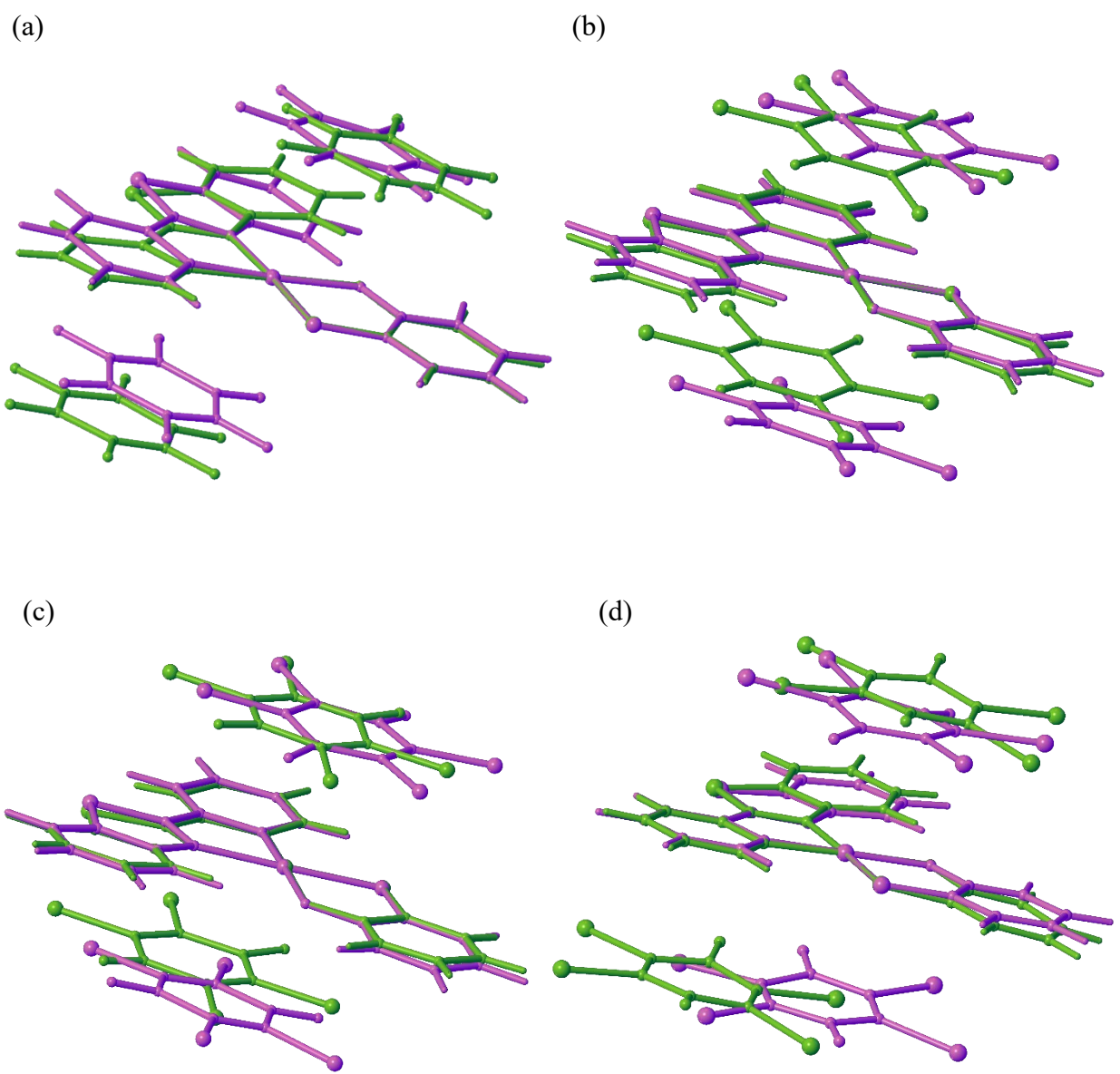


Figure S34. Overlayed images of **1·QF** (a) **1·QCl** (b), **1·QBr** (c) and **1·QI** (d) in X-ray (green) and optimized trimolecular model (purple) geometries.

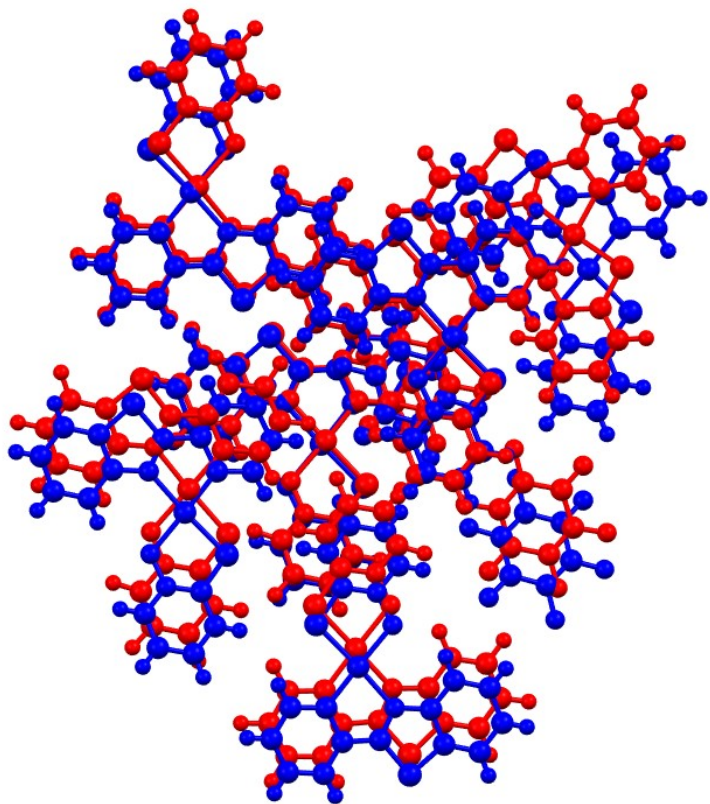


Figure S35. Overlayed images of the optimized and experimental X-ray geometries of **1**·QF (an octa-molecular cluster bearing 6 molecules of **1** and 2 molecules of QF).

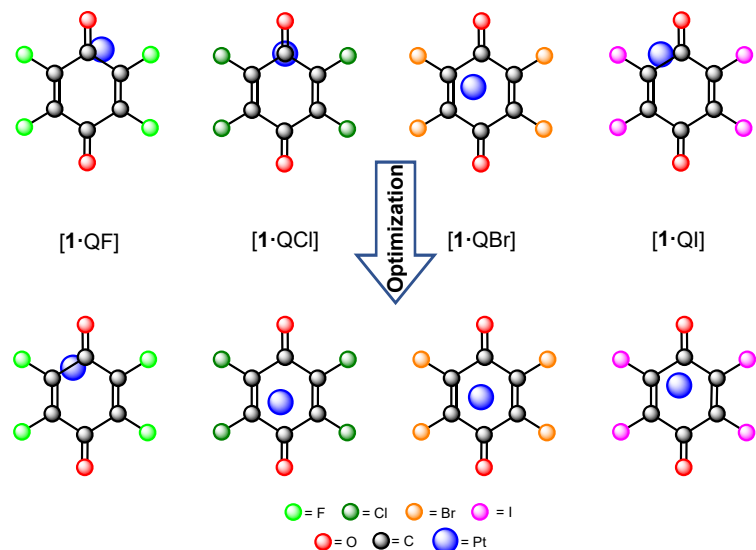


Figure S36. Projections of Pt centers (in blue) onto the mean-square planes of the closest QX rings in the cocrystals from the XRD data (top panel) and in the optimization of dimeric adducts (bottom panel) $[1\cdot QX]$.

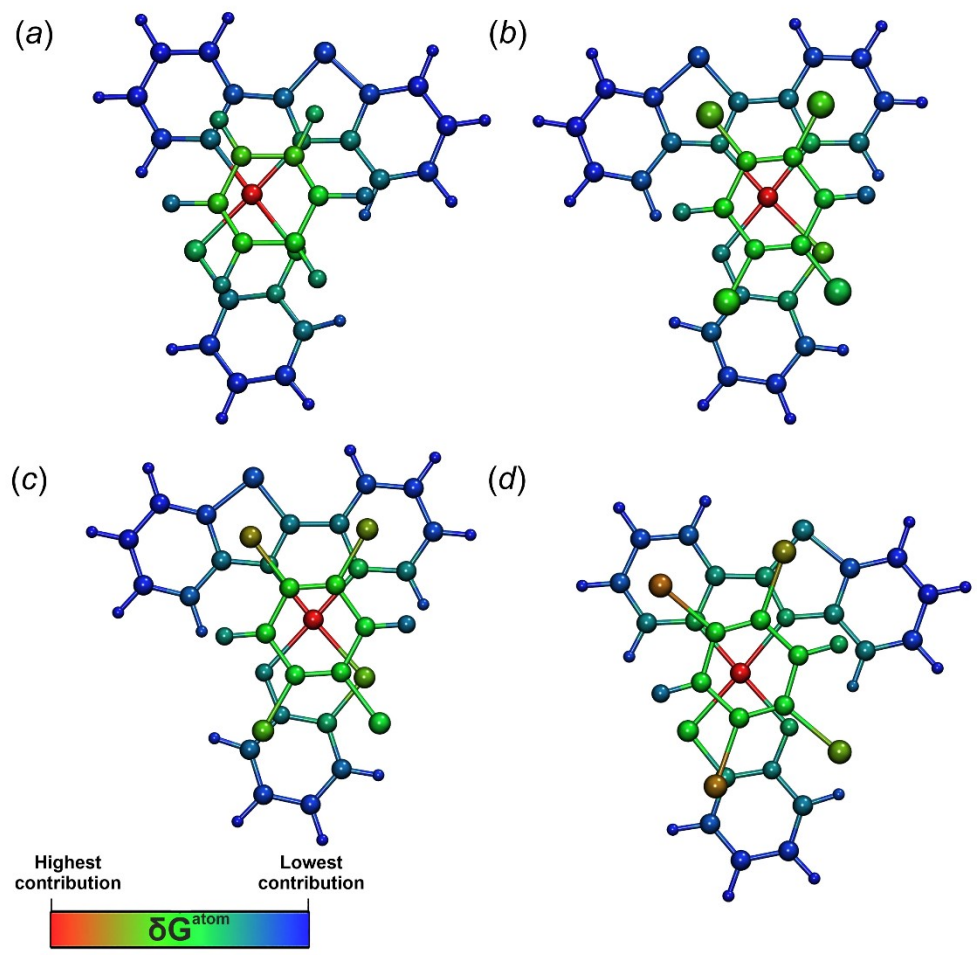


Figure S37. The δG^{atom} colored $[1 \cdot \text{QX}]$ structures.

Table S7. Geometrical parameters of the observed noncovalent interactions in the crystal and optimized structures.

Structure	Contact	$d(X \cdots Y)$, Å	$\Sigma_{Wdv}^{Alvarez}(X \cdots Y)$, Å	R_r	QX-square plane angle, °	$d1$, Å	$d2$, Å	$d3$, Å	r , Å	α , °
X-ray										
1·QF	Pt1···C1D	3.320(3)	4.06	0.82	4.62(15)	3.6366(13)	3.276(2)	3.3522(17)	1.578	25.7
	Pt1···C2D	3.426(3)	4.06	0.84						
	Pt1···C3D	4.002(3)	4.06	0.99						
	Pt1···C4D	4.421(3)	4.06	1.09						
	Pt1···C5D	4.308(3)	4.06	1.06						
	Pt1···C6D	3.837(3)	4.06	0.95						
	C18···O2D	3.326(5)	3.27	0.99						
	O1···C4D	3.262(4)	3.27	1.00						
	N1···C2D	3.615(4)	3.43	1.05						
	C12···F2D	3.205(4)	3.23	0.99						
	C13···F1D	3.386(3)	3.23	1.05						
	C14···F3D	3.531(4)	3.23	1.09						
Optimized										
	Pt1···C1D	3.323	4.06	0.82	5.42	3.396	3.269	3.542	0.920	15.7
	Pt1···C2D	3.632	4.06	0.89						

	Pt1···C3D	3.966	4.06	0.98						
	Pt1···C4D	4.025	4.06	0.99						
	Pt1···C5D	3.739	4.06	0.92						
	Pt1···C6D	3.369	4.06	0.83						
	C18···O2D	3.161	3.27	0.97						
	O1···C4D	3.075	3.27	0.94						
	N1···C2D	3.255	3.43	0.95						
	C12···F2D	3.289	3.23	1.02						
	C13···F1D	3.204	3.23	0.99						
	C14···F3D	3.282	3.23	1.02						
X-ray										
1·QCl	Pt1···C1D	3.504(9)	4.06	0.86	5.45(41)	3.627(4)	3.449(6)	3.896(5)	1.222	18.0
	Pt1···C2D	3.634(10)	4.06	0.90						
	Pt1···C3D	4.071(9)	4.06	1.00						
	Pt1···C4D	4.328(10)	4.06	1.06						
	Pt1···C5D	4.079(8)	4.06	1.00						
	Pt1···C6D	3.735(10)	4.06	0.92						
	C18···Cl3D	3.347(9)	3.59	0.93						
	C13···Cl2D	3.542(10)	3.59	0.99						

	C6···Cl1D	3.569(9)	3.59	0.99						
	N1···Cl2D	3.915(9)	3.48	1.13						
	C7···Cl2D	4.142(10)	3.59	1.15						
	S2···C6D	3.987(11)	3.66	1.09						
	Optimized									
	Pt1···C1D	3.798	4.06	0.94						
	Pt1···C2D	3.651	4.06	0.90						
	Pt1···C3D	3.562	4.06	0.88						
	Pt1···C4D	3.612	4.06	0.89						
	Pt1···C5D	3.837	4.06	0.95						
	Pt1···C6D	3.914	4.06	0.96						
	C18···Cl3D	3.480	3.59	0.97						
	C13···Cl2D	3.606	3.59	1.01						
	C6···Cl1D	3.658	3.59	1.02						
1·QBr	X-ray									
	Pt1···C1D	3.896(8)	4.06	0.96	1.81(25)	3.467(3)	3.450(3)	4.006(4)	0.342	5.7

Pt1···C2D	3.850(8)	4.06	0.95						
Pt1···C3D	3.727(9)	4.06	0.92						
Pt1···C4D	3.644(9)	4.06	1.63						
Pt1···C5D	3.648(8)	4.06	0.90						
Pt1···C6D	3.752(7)	4.06	0.92						
C2···O2D	3.994(10)	3.27	1.22						
C12···O1D	3.300(11)	3.27	1.01						
N1···Br1D	3.839(7)	3.52	1.09						
N2···Br4D	3.873(7)	3.52	1.10						
C13···Br1D	3.974(8)	3.63	1.09						
C7···Br1D	3.615(8)	3.63	0.99						
C1···Br2D	3.748(8)	3.63	1.03						
C18···Br4D	3.843(9)	3.63	1.06						
S2···Br3D	3.8814(18)	3.75	1.03						
S2···C4D	3.840(9)	3.66	1.05						
Optimized									
Pt1···C1D	3.652	4.06	0.90	0.60	3.470	3.438	3.718	0.463	7.8
Pt1···C2D	3.600	4.06	0.87						
Pt1···C3D	3.663	4.06	0.90						

	Pt1···C4D	3.785	4.06	0.93						
	Pt1···C5D	3.937	4.06	0.97						
	Pt1···C6D	3.885	4.06	0.96						
	C2···O2D	3.697	3.27	1.13						
	C12···O1D	3.567	3.27	1.09						
	N1···Br1D	3.612	3.52	1.03						
	N2···Br4D	3.599	3.52	1.02						
	C13···Br1D	3.646	3.63	1.00						
	C7···Br1D	3.742	3.63	1.03						
	C1···Br2D	3.713	3.63	1.02						
	C18···Br4D	3.586	3.63	0.99						
	S2···Br3D	3.884	3.75	1.04						
	S2···C4D	3.684	3.66	1.01						
1·QI	X-ray									
	Pt1···C1D	4.698(12)	4.06	1.16	3.1(3)	3.928(4)	3.602(8)	4.392(6)	1.566	23.5
	Pt1···C2D	4.206(11)	4.06	1.04						
	Pt1···C3D	3.717(10)	4.06	0.92						
	Pt1···C4D	3.707(11)	4.06	0.91						
	Pt1···C5D	4.103(10)	4.06	1.01						

Pt1···C6D	4.561(11)	4.06	1.12								
C12···O1D	3.753(15)	3.27	1.15								
C13···O1D	4.285(15)	3.27	1.31								
C7···I1D	4.082(11)	3.81	1.07								
C18···I4D	4.614(12)	3.81	1.21								
C3···I2D	4.304(11)	3.81	1.13								
C14···I3D	3.672(11)	3.81	0.96								
C15···I3D	3.869(12)	3.81	1.02								
H12···I4D	4.1904(7)	3.24	1.29								
S1···I1D	3.946(3)	3.93	1.00								
S2···I3D	4.427(3)	3.93	1.13								
Optimized											
Pt1···C1D	3.862	4.06	0.95	3.62							
Pt1···C2D	3.879	4.06	0.96								
Pt1···C3D	3.764	4.06	0.93								
Pt1···C4D	3.636	4.06	0.90								
Pt1···C5D	3.703	4.06	0.91								
Pt1···C6D	3.794	4.06	0.93								
C12···O1D	3.279	3.27	1.00								

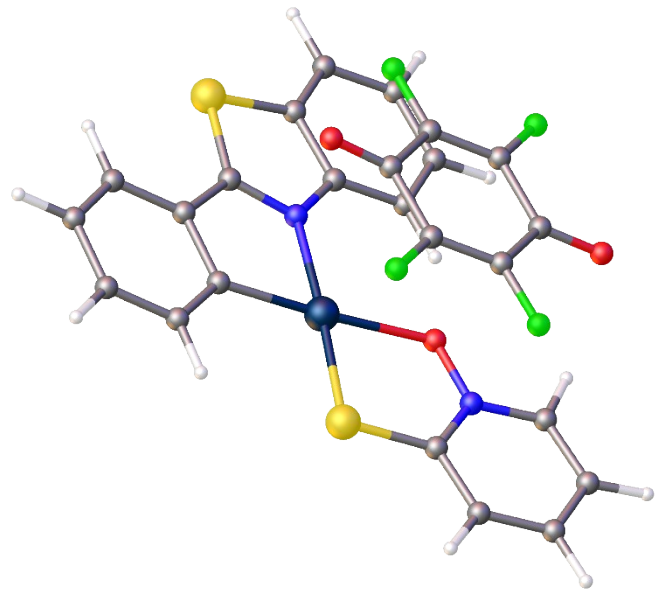
C13···O1D	3.447	3.27	1.05					
O1···I4D	3.764	3.54	1.06					
C7···I1D	3.839	3.81	1.10					
C18···I4D	3.898	3.81	1.02					
C3···I2D	3.916	3.81	1.03					
C14···I3D	3.694	3.81	0.97					
C15···I3D	3.902	3.81	1.02					
H12···I4D	3.688	3.24	1.14					
S1···I1D	3.934	3.93	1.00					
S2···I3D	4.098	3.93	1.04					

S5. CARTESIAN COORDINATES FOR THE STUDIED MOLECULES

Optimized geometries

Cartesian coordinate for [1·QF] (in Å)

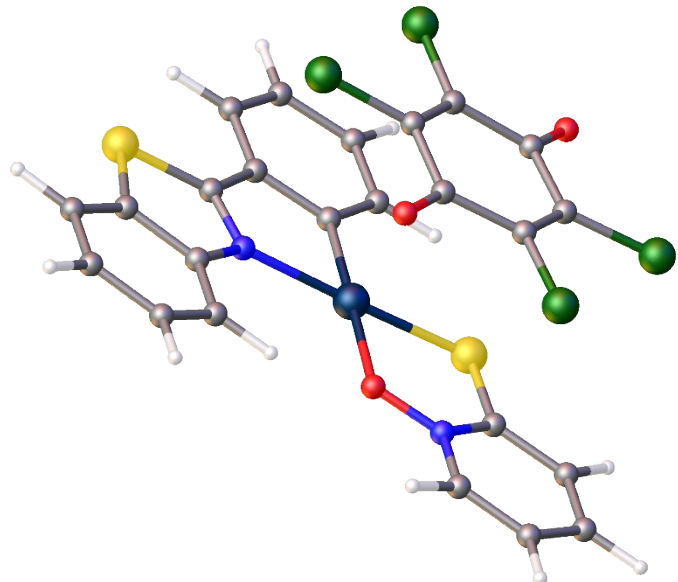
Pt	0.000000	2.100980	0.000000
S	4.086866	3.926284	0.052870
S	-2.233801	1.874314	0.003797
O	0.000000	0.000000	0.000000
N	2.029577	2.399726	-0.048736
N	-1.197814	-0.576811	0.026121
C	2.384449	3.664884	0.063313
C	1.344083	4.642106	0.164002
C	3.072230	0.168600	-0.320241
H	2.118317	-0.339845	-0.361132
C	0.050459	4.072862	0.115987
C	5.492746	0.156639	-0.360142
H	6.416124	-0.404715	-0.433046
C	3.110426	1.550918	-0.169660
C	4.269470	-0.513134	-0.412315
H	4.257994	-1.590405	-0.524787
C	1.555854	6.012719	0.295268
H	2.565369	6.409225	0.335283
C	-1.217789	-1.925709	0.076979
H	-0.239499	-2.381110	0.103831
C	-3.554567	-0.523483	0.054004
H	-4.458619	0.070805	0.052211
C	5.542727	1.531116	-0.218541
H	6.490080	2.054084	-0.180658
C	4.342858	2.218782	-0.125709
C	0.470415	6.858858	0.378519
H	0.615167	7.926860	0.483432
C	-2.397330	-2.610909	0.111181
H	-2.377908	-3.690320	0.159490
C	-0.813889	6.324097	0.329695
H	-1.670110	6.986405	0.396964
C	-1.021265	4.959421	0.201948
H	-2.039050	4.587437	0.176058
C	-2.333923	0.162341	0.024045
C	-3.595034	-1.892251	0.096059



H	-4.546301	-2.408235	0.124874
F	3.037774	1.969246	3.006076
F	-1.968869	-0.231592	3.261444
F	2.718578	-0.745130	2.819054
F	-1.652709	2.480740	3.449229
O	0.853583	3.487544	3.425596
O	0.224057	-1.749962	2.884222
C	-0.783571	0.345458	3.207013
C	1.853594	1.397440	3.043418
C	0.363642	-0.555132	3.002417
C	-0.636537	1.670718	3.280731
C	1.698835	0.075339	2.956006
C	0.702375	2.307510	3.241357

Cartesian coordinate for [1·QCl] (in Å)

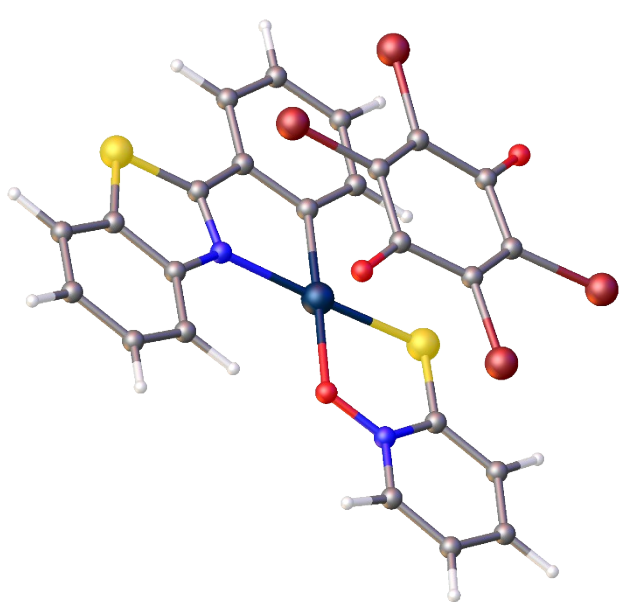
Pt	0.000000	0.000000	0.000000
S	0.000000	2.242416	0.000000
S	1.431305	-4.242444	0.034989
N	0.098885	-2.051497	0.001737
C	2.406759	-1.580268	0.036161
O	-2.082756	0.207406	-0.020784
C	-3.023746	-4.013255	-0.172229
H	-4.099145	-3.902756	-0.240054
C	1.960489	-0.238289	0.004865
C	3.756952	-1.922414	0.025685
H	4.057690	-2.965160	0.046596
C	-1.690830	2.511211	-0.069275
C	1.328862	-2.522594	0.035731
N	-2.536742	1.451406	-0.063032
C	4.295064	0.405709	-0.057970
H	5.038220	1.194140	-0.104186
C	-4.443259	2.845487	-0.178552
H	-5.519941	2.931534	-0.220004
C	-3.876642	1.605361	-0.113304
H	-4.425602	0.675494	-0.107701
C	-2.253095	3.792336	-0.141075
H	-1.571517	4.632414	-0.155366
C	2.950662	0.742587	-0.043518
H	2.677754	1.790799	-0.084376
C	4.707142	-0.923534	-0.021226



H	5.761491	-1.170534	-0.033400
C	-2.468612	-5.293908	-0.146767
H	-3.115981	-6.161289	-0.188764
C	-0.852552	-3.049816	-0.043939
C	-2.231295	-2.884347	-0.121088
H	-2.649204	-1.887805	-0.153476
C	-0.300683	-4.339017	-0.028381
C	-3.610642	3.967521	-0.195674
H	-4.030322	4.963690	-0.253651
C	-1.099537	-5.471049	-0.076059
H	-0.664437	-6.462532	-0.063091
Cl	-0.603880	3.467238	-3.554001
Cl	2.834988	-0.677783	-3.482489
Cl	0.381876	-2.712108	-3.415147
C	1.006645	1.302710	-3.422133
C	0.184524	-1.023545	-3.407335
O	1.930137	2.071738	-3.407403
C	-1.431923	0.926277	-3.437632
Cl	-3.056165	1.432809	-3.490980
C	1.217890	-0.170191	-3.438181
C	-1.220958	-0.543735	-3.356245
O	-2.147632	-1.307172	-3.278489
C	-0.402864	1.782840	-3.461281

Cartesian coordinate for [1·QBr] (in Å)

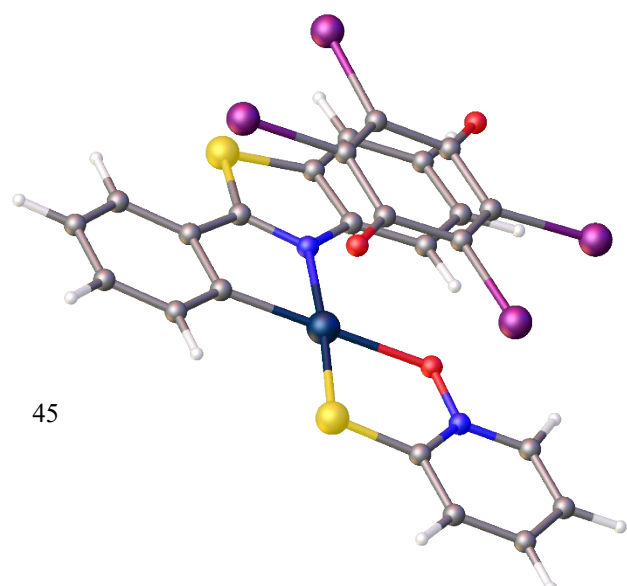
Pt	0.000000	0.000000	0.000000
S	-0.082223	-4.244611	1.423191
S	0.000000	2.242416	0.000000
O	0.009144	0.207190	-2.081960
N	0.022140	1.451162	-2.537369
C	0.140254	-2.881619	-2.234108
H	0.188127	-1.884798	-2.649872
N	-0.010682	-2.051597	0.095421
C	0.075678	3.792931	-2.256016
H	0.095512	4.633445	-1.575230
C	0.033589	2.511268	-1.691849
C	0.033038	0.736838	2.952513
H	0.091233	1.784785	2.681918
C	0.035149	1.604899	-3.878040
H	0.028042	0.674595	-4.426218



C	0.026038	0.397398	4.296251
H	0.073727	1.183717	5.041547
C	0.002699	-4.338701	-0.307932
C	-0.081478	-1.928664	3.752940
H	-0.119727	-2.971605	4.051331
C	-0.069039	-1.584056	2.403405
C	-0.064283	-2.524525	1.324008
C	-0.016079	-0.241648	1.959890
C	0.038006	-3.048750	-0.857200
C	0.197308	-4.009829	-3.027348
H	0.285737	-3.897772	-4.101086
C	0.055784	-5.469840	-1.107692
H	0.027841	-6.461833	-0.674386
C	0.152183	-5.291125	-2.475071
H	0.199399	-6.157800	-3.123055
C	0.091300	3.967995	-3.614615
H	0.123897	4.964737	-4.035658
C	-0.034186	-0.931985	4.705470
H	-0.039814	-1.180745	5.759493
C	0.066548	2.845654	-4.446406
H	0.076732	2.931829	-5.523835
Br	3.556769	1.588478	-3.201738
Br	3.505128	-2.866049	0.254333
Br	3.525186	-0.785769	2.934757
Br	3.574633	3.669181	-0.522700
O	3.352798	2.027248	1.959647
O	3.294546	-1.216809	-2.224176
C	3.411583	1.289524	1.012695
C	3.470911	0.993149	-1.436075
C	3.473175	1.815218	-0.381566
C	3.454822	-1.008696	0.116156
C	3.387662	-0.484469	-1.273984
C	3.464724	-0.190412	1.175415

Cartesian coordinate for [1·QI] (in Å)

Pt	0.000000	0.000000	0.000000
S	2.225312	0.222252	0.154052
S	-4.020781	-1.834305	-0.711511
O	0.000000	2.093451	0.000000
N	1.191710	2.668446	0.075137



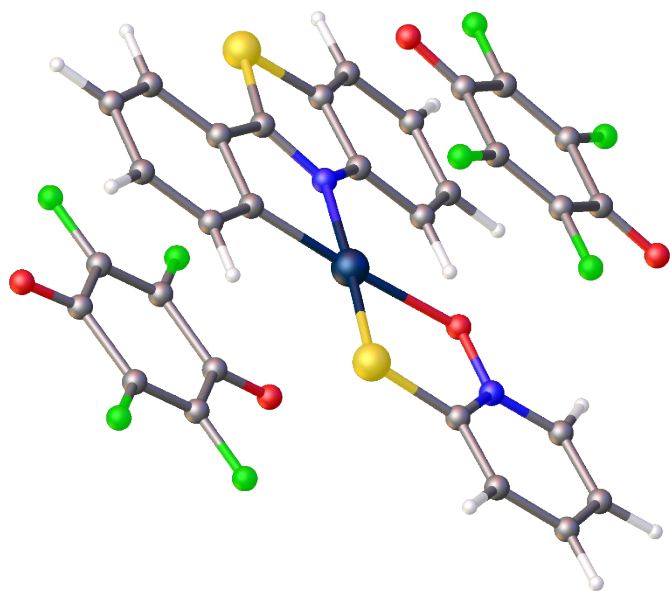
C -0.041593 -1.973283 -0.025669
 C -3.086065 1.934315 -0.254518
 H -2.156535 2.446224 -0.046708
 N -2.020520 -0.302116 -0.232803
 C -0.441441 -4.774483 -0.126978
 H -0.579770 -5.848089 -0.160119
 C -1.317084 -2.549990 -0.234994
 C 2.327485 1.931059 0.141292
 C -1.519013 -3.927470 -0.283164
 H -2.515503 -4.329335 -0.436273
 C 1.021805 -2.862489 0.129861
 H 2.023363 -2.486802 0.304716
 C 0.825011 -4.233362 0.077752
 H 1.674138 -4.895692 0.206861
 C 3.546029 2.618938 0.216276
 H 4.448104 2.023872 0.268819
 C 1.212616 4.018370 0.092247
 H 0.234400 4.471715 0.038747
 C -5.471823 1.939122 -0.663487
 H -6.392722 2.499098 -0.770854
 C -2.352853 -1.570352 -0.371321
 C -4.278003 2.613629 -0.402343
 H -4.288376 3.692447 -0.305988
 C 2.388802 4.706199 0.170124
 H 2.368831 5.786777 0.181592
 C -4.301584 -0.123477 -0.631580
 C -5.496911 0.562158 -0.781726
 H -6.421938 0.035494 -0.980085
 C -3.099056 0.548376 -0.369149
 C 3.586199 3.987928 0.232055
 H 4.535426 4.505020 0.292720
 I -0.484970 -3.296450 3.647330
 I -1.050499 3.680409 3.247471
 I -3.738644 -1.634889 3.207491
 I 2.198353 2.031927 3.831217
 O 1.596054 -1.000171 3.699784
 O -3.083644 1.376282 2.976745
 C -0.772285 1.625285 3.340161
 C 0.528168 -0.462297 3.567299
 C -2.025805 0.835342 3.180187
 C -1.919849 -0.643085 3.308700

C -0.736177 -1.249738 3.473023

C 0.409291 1.027218 3.534181

Cartesian coordinate for [1·(QF)₂] (in Å)

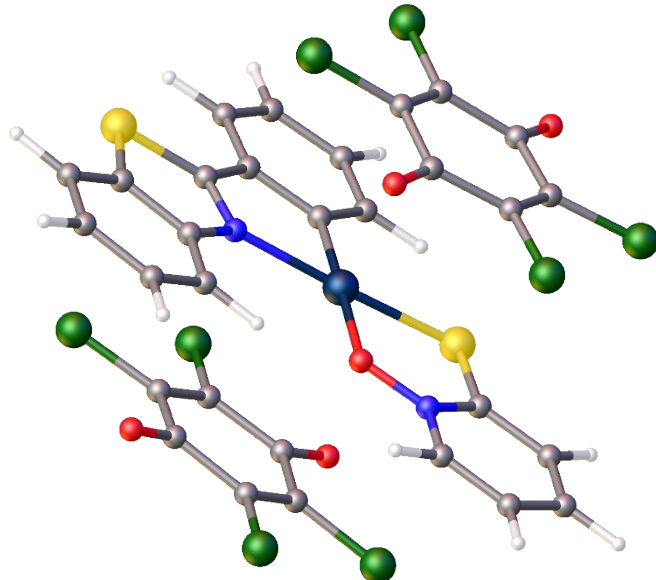
Pt	0.000000	0.000000	0.000000
S	0.000000	2.246287	0.000000
S	-1.393005	-4.242669	-0.270894
O	2.068810	0.205188	0.222859
N	-0.101068	-2.048634	0.017122
N	2.517121	1.452530	0.334522
C	-1.936376	-0.239548	-0.304878
C	-1.303472	-2.525572	-0.247948
C	-2.366551	-1.583501	-0.426478
C	2.163567	-2.868012	0.596430
H	2.559758	-1.869332	0.719855
C	-2.916654	0.742589	-0.436186
H	-2.652616	1.790650	-0.354758
C	0.827970	-3.041929	0.251277
C	2.939520	-3.993869	0.784332
H	3.982087	-3.879694	1.054382
C	1.676283	2.511038	0.255995
C	2.230182	3.790994	0.373566
H	1.554547	4.633699	0.312369
C	0.294503	-4.332053	0.121773
C	-4.241792	0.404784	-0.660317
H	-4.983336	1.191395	-0.740940
C	3.847758	1.600633	0.502849
H	4.396661	0.671436	0.521904
C	-3.696700	-1.924132	-0.661923
H	-3.989140	-2.965685	-0.743489
C	1.077306	-5.460122	0.309362
H	0.659827	-6.453642	0.205438
C	2.407160	-5.276045	0.638602
H	3.041207	-6.140580	0.792129
C	-4.639006	-0.924363	-0.774514
H	-5.679621	-1.170653	-0.942269
C	3.577750	3.961994	0.554883
H	3.992766	4.957901	0.643691
C	4.406752	2.840160	0.618758
H	5.476095	2.925205	0.749551
F	1.097726	-3.183234	-2.889538
F	3.635009	-2.299697	-2.341326
F	2.222709	2.173410	-2.981645



F	-0.316664	1.293543	-3.519465
O	-0.786653	-1.363483	-3.498083
O	4.103319	0.348451	-2.371136
C	1.413150	-1.906365	-2.885597
C	2.648167	-1.477126	-2.621917
C	1.903972	0.894987	-2.982475
C	2.988928	-0.038484	-2.630564
C	0.661425	0.471982	-3.227315
C	0.316043	-0.969607	-3.216956
F	-3.368830	-2.934058	2.636233
F	-0.706178	-3.291999	3.145743
F	-0.125696	1.401791	3.416614
F	-2.788591	1.762764	2.889842
O	-4.344916	-0.423479	2.595836
O	0.831134	-1.115308	3.535473
C	-2.550698	-1.920561	2.824533
C	-1.251406	-2.095285	3.073521
C	-0.944238	0.393740	3.213459
C	-0.338441	-0.953154	3.290201
C	-2.245881	0.567855	2.970300
C	-3.161416	-0.573692	2.768861

Cartesian coordinate for [1·(QCl)₂] (in Å)

Pt	-0.003009	-0.001594	-0.009122
S	-2.230494	-0.262501	0.025764
S	4.038342	1.912517	-0.209882
N	2.023543	0.334704	-0.077184
C	1.286375	2.572026	-0.045586
O	0.036837	-2.091278	-0.009053
C	4.329906	-2.542859	-0.240625
H	4.345313	-3.625681	-0.252262
C	0.005324	1.974510	-0.006251
C	1.467687	3.952466	-0.045671
H	2.467823	4.372988	-0.073242
C	-2.297440	-1.975216	0.012244
C	2.347775	1.611976	-0.099875
N	-1.146485	-2.689468	0.008541
C	-0.908608	4.215842	0.019637
H	-1.779150	4.861856	0.041884
C	-2.305295	-4.748382	0.020183

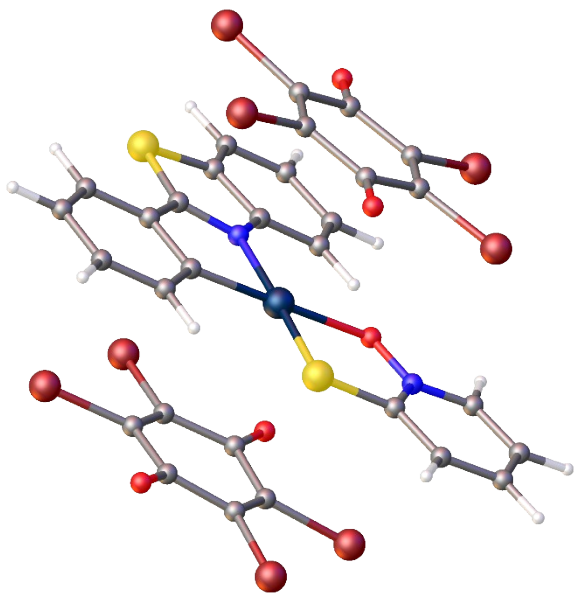


H -2.265015 -5.828474 0.025659
 C -1.139489 -4.038665 0.016585
 H -0.150760 -4.472138 0.010724
 C -3.504394 -2.684620 0.009439
 H -4.419171 -2.107150 0.006514
 C -1.085596 2.841052 0.024209
 H -2.094816 2.446951 0.050896
 C 0.363590 4.779266 -0.012409
 H 0.485707 5.855311 -0.012845
 C 5.534517 -1.841192 -0.308695
 H 6.469607 -2.384288 -0.370211
 C 3.123450 -0.496969 -0.147597
 C 3.118968 -1.886970 -0.159387
 H 2.181105 -2.421438 -0.109147
 C 4.336192 0.202336 -0.220765
 C -3.517693 -4.054536 0.014301
 H -4.458208 -4.590507 0.012248
 C 5.551529 -0.459225 -0.300789
 H 6.483668 0.088931 -0.355538
 Cl -3.487930 -1.059031 -3.439367
 Cl 0.308197 2.761237 -3.521853
 Cl 2.569486 0.513390 -3.517721
 C -1.484792 0.752449 -3.393722
 C 0.909236 0.155970 -3.450284
 O -2.337633 1.598588 -3.366381
 C -0.876936 -1.639569 -3.395335
 Cl -1.227463 -3.305368 -3.407734
 C -0.039801 1.103019 -3.455536
 C 0.567810 -1.287886 -3.363651
 O 1.418630 -2.135262 -3.289989
 C -1.828550 -0.697157 -3.402906
 Cl -2.540654 -1.779121 3.541520
 Cl 0.063439 2.938513 3.549782
 Cl 2.845190 1.400216 3.311860
 C -1.116241 0.514192 3.478969
 C 1.345314 0.601151 3.341861
 O -2.167049 1.091305 3.561283
 C 0.119478 -1.616402 3.313695
 Cl 0.239754 -3.311594 3.247226
 C 0.177073 1.250082 3.446011
 C 1.408135 -0.878627 3.227697

O	2.454086	-1.456861	3.088854
C	-1.048737	-0.973030	3.434890

Cartesian coordinate for [1·(QBr)₂] (in Å)

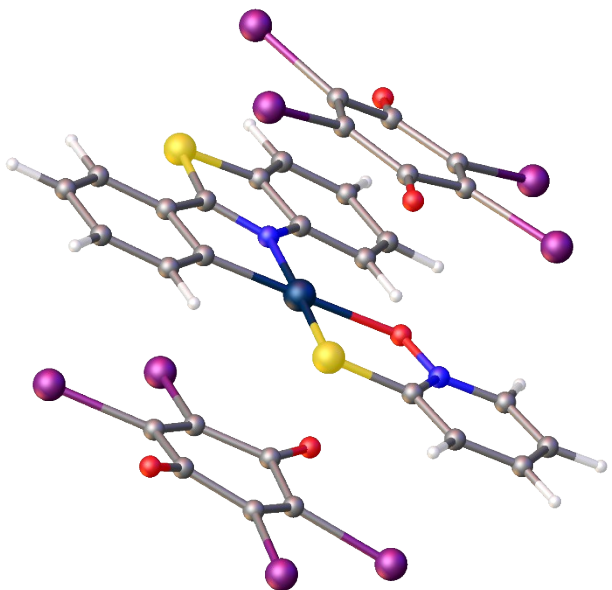
Pt	0.033934	2.449488	-0.026550
S	-3.999926	4.336122	-0.481744
S	2.232419	2.192656	0.326261
O	0.039937	0.376405	-0.283050
N	1.219467	-0.215883	-0.158757
C	-3.021970	0.555639	-0.636824
H	-2.086582	0.028002	-0.516455
N	-1.972075	2.778229	-0.326353
C	3.538494	-0.211386	0.267385
H	4.423449	0.359832	0.513643
C	2.334944	0.492940	0.139165
C	1.029086	5.268295	0.532862
H	2.025917	4.874305	0.692704
C	1.247489	-1.549935	-0.353469
H	0.285850	-1.979413	-0.591074
C	0.822692	6.631852	0.671378
H	1.659250	7.269992	0.933600
C	-4.261195	2.632869	-0.677721
C	-1.498253	6.376683	0.153413
H	-2.487963	6.796082	0.004417
C	-1.290364	5.005669	0.025494
C	-2.319244	4.048875	-0.255298
C	-0.019117	4.410688	0.203462
C	-3.047435	1.942872	-0.551022
C	-4.211678	-0.106203	-0.860470
H	-4.212066	-1.187380	-0.925422
C	-5.453925	1.965790	-0.907781
H	-6.386162	2.506578	-1.011089
C	-5.414870	0.587380	-1.000412
H	-6.332537	0.040475	-1.179172
C	3.586472	-1.567278	0.077493
H	4.524437	-2.098605	0.176560
C	-0.435475	7.194454	0.478387
H	-0.579784	8.262498	0.584302
C	2.412705	-2.252931	-0.245409
H	2.400933	-3.321422	-0.408014



Br	-1.045516	-0.033036	-3.806495
Br	-2.169361	5.496874	-3.692241
Br	1.102768	6.151239	-3.125161
Br	2.258923	0.636891	-3.422184
O	2.605576	3.575970	-3.095147
O	-2.553089	2.537393	-3.746820
C	1.436882	3.341941	-3.247687
C	-0.363053	1.687146	-3.599752
C	0.937595	1.949991	-3.430242
C	-0.872594	4.168924	-3.520906
C	-1.378611	2.775661	-3.630212
C	0.422851	4.432354	-3.310321
Br	0.764847	-1.399341	3.207648
Br	-3.299280	2.504090	3.016314
Br	-1.019686	4.913523	3.726825
Br	3.044960	1.008425	3.925916
O	1.685651	3.663028	3.844444
O	-1.865917	-0.093127	2.693088
C	0.867712	2.804805	3.647496
C	0.349908	0.416911	3.298849
C	1.251135	1.365046	3.576759
C	-1.477854	2.169482	3.217993
C	-1.075613	0.750190	3.028014
C	-0.580510	3.121795	3.501105

Cartesian coordinate for [1·(QI)₂] (in Å)

Pt	0.311453	-0.391877	-0.082367
S	-1.916454	-0.177342	-0.228514
S	4.406378	-2.192679	-0.034014
O	0.269467	1.642623	0.388114
N	-0.930699	2.204358	0.419263
C	0.398019	-2.318207	-0.512802
C	3.350366	1.532307	0.496570
H	2.398637	2.042894	0.462594
N	2.340025	-0.680257	0.030129
C	0.864023	-5.052508	-1.069362
H	1.027415	-6.101324	-1.284249
C	1.693587	-2.884847	-0.487493
C	-2.049236	1.492000	0.136739
C	1.927237	-4.230235	-0.758165

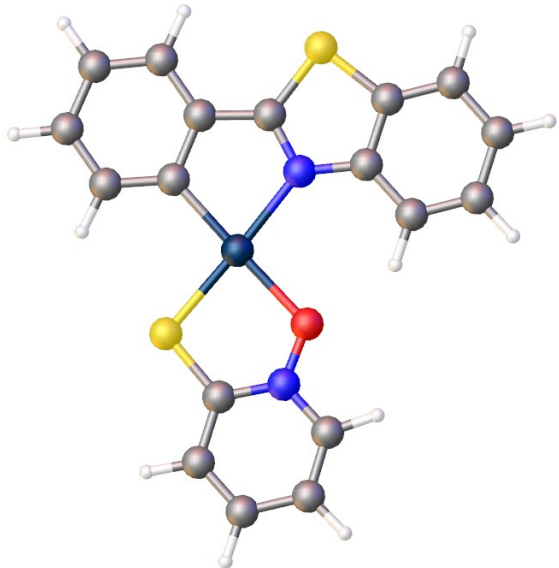


H 2.937276 -4.626156 -0.727005
 C -0.650335 -3.178834 -0.836581
 H -1.666733 -2.805800 -0.884728
 C -0.420347 -4.518179 -1.109887
 H -1.258396 -5.158379 -1.362024
 C -3.275057 2.167665 0.161105
 H -4.161860 1.593467 -0.070490
 C -0.977452 3.512681 0.743290
 H -0.012059 3.948435 0.951041
 C 5.757803 1.534640 0.747944
 H 6.670137 2.089244 0.930222
 C 2.712720 -1.927588 -0.174410
 C 4.533596 2.204891 0.722303
 H 4.511943 3.276564 0.878064
 C -2.164651 4.185953 0.783671
 H -2.166062 5.234389 1.046409
 C 4.637327 -0.507078 0.304778
 C 5.823995 0.170289 0.536344
 H 6.772455 -0.351821 0.549046
 C 3.403780 0.158799 0.290495
 C -3.341346 3.498768 0.479277
 H -4.296586 4.007684 0.495991
 I -1.573735 -4.117777 2.856770
 I 1.340959 2.174038 3.888307
 I 2.072562 -3.693505 3.152311
 I -2.320201 1.695142 3.943453
 O -2.747429 -1.276739 3.220663
 O 2.506877 -0.627549 3.300579
 C 0.386054 0.361418 3.565935
 C -1.553120 -1.141998 3.293273
 C 1.313573 -0.787221 3.344367
 C 0.702334 -2.139865 3.214290
 C -0.626692 -2.300321 3.147637
 C -0.941456 0.190223 3.571186
 I 1.188817 -2.655230 -4.276812
 I -0.821050 3.914597 -2.947589
 I 3.620253 -0.004450 -3.451991
 I -3.262956 1.255961 -3.721705
 O -1.589865 -1.351526 -3.838386
 O 1.882926 2.430709 -2.627694
 C -0.338960 1.913093 -3.211166

C	-0.789339	-0.465606	-3.689635
C	1.110567	1.604471	-3.042607
C	1.561171	0.241664	-3.440189
C	0.679885	-0.722735	-3.739518
C	-1.224955	0.950156	-3.493608

Cartesian coordinate for 1 (in Å)

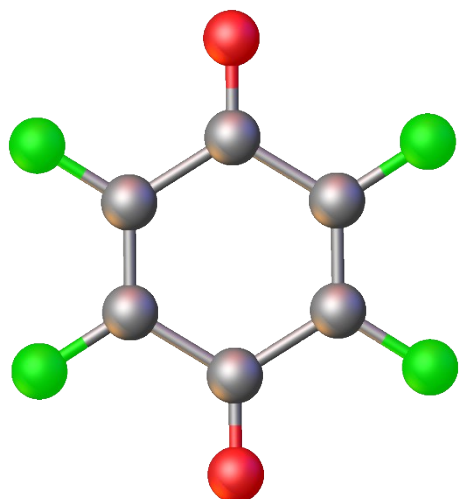
Pt	2.141438669	5.440252825	5.475395509
S	1.662350368	3.539538592	6.563184049
S	4.316401298	9.087482667	4.055496974
O	0.239739306	5.195750783	4.638125659
N	-0.413882123	4.103800437	5.003306375
N	2.658388253	7.186326682	4.528810266
C	4.633437952	6.849391596	5.767610541
C	-1.626749834	3.905464264	4.443366076
H	-1.920641463	4.678724234	3.749034543
C	2.300730266	10.061224984	2.349045166
H	2.900656368	10.915764459	2.061863997
C	3.949941860	5.695412972	6.218995332
C	-1.876064357	1.883360732	5.669762815
H	-2.448665637	1.003626602	5.934801354
C	-0.644408019	2.099663536	6.228247239
H	-0.215802559	1.405920619	6.939480771
C	4.642260383	4.882867037	7.118260795
H	4.179216956	3.980386612	7.500868286
C	1.032884309	9.874200541	1.830918243
H	0.634065664	10.593934844	1.126510150
C	3.861920858	7.621049501	4.842064368
C	0.116200562	3.229982648	5.896782988
C	0.264335258	8.770410149	2.204759552
H	-0.726150466	8.647290224	1.783295307
C	0.739510074	7.832329125	3.099931866
H	0.153595583	6.973280581	3.397612277
C	2.780862187	9.121186543	3.247778574
C	-2.380459366	2.810561403	4.753022801
H	-3.345589972	2.684226185	4.282968835
C	2.014656165	8.009456365	3.628228329
C	5.923255046	5.202875876	7.538681561
H	6.431028161	4.547773697	8.238432023
C	5.921605021	7.175151685	6.188554979



H	6.409439405	8.070578296	5.816109535
C	6.570821548	6.347651747	7.080053800
H	7.572172279	6.583600956	7.418339064

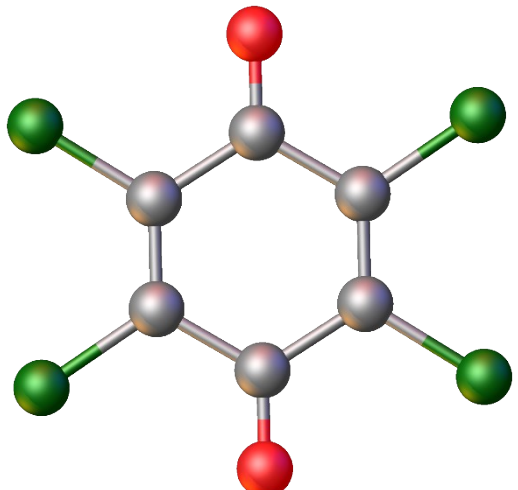
Cartesian coordinate for QF (in Å)

F	1.032450000	5.806982000	-1.522971000
F	1.151448000	3.610013000	0.111953000
O	3.147063000	7.473305000	-1.582492000
C	2.078169000	5.544312000	-0.773473000
C	2.136010000	4.474233000	0.023096000
C	3.198389000	6.509283000	-0.863335000
F	5.488856000	4.894609000	1.522959000
F	5.369858000	7.091578000	-0.111965000
O	3.374245000	3.228285000	1.582477000
C	4.443129000	5.157291000	0.773477000
C	4.385288000	6.227370000	-0.023092000
C	3.322895000	4.192339000	0.863366000



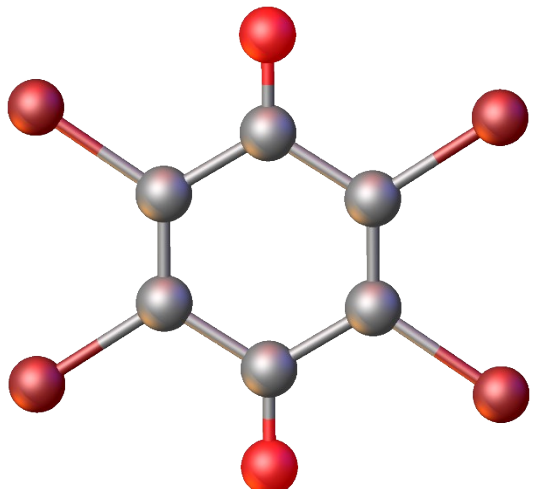
Cartesian coordinate for QCl (in Å)

Cl	1.274016000	7.477191000	2.239551000
Cl	3.541111000	5.305604000	1.668837000
Cl	-2.514914000	3.723196000	1.471937000
Cl	-0.247824000	1.551460000	0.901968000
O	-1.369529000	6.317605000	2.045279000
O	2.395764000	2.710882000	1.096793000
C	1.882684000	4.942805000	1.631602000
C	0.929704000	5.855572000	1.871561000
C	-0.515371000	5.499433000	1.829870000
C	1.541613000	3.529139000	1.311779000
C	-0.856444000	4.085929000	1.509634000
C	0.096486000	3.173041000	1.269902000



Cartesian coordinate for QBr (in Å)

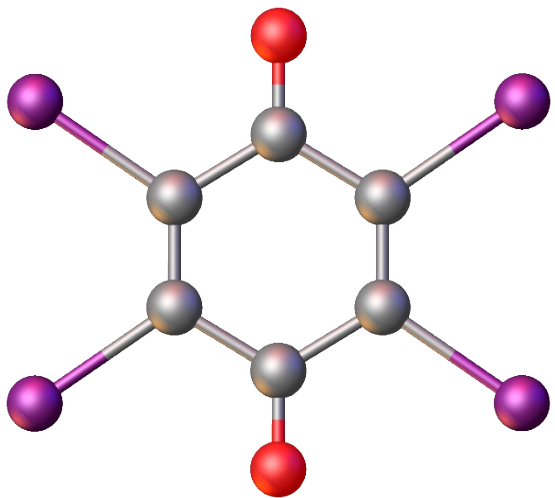
Br	1.290986000	7.636166000	2.275684000
Br	3.703714000	5.325254000	1.668806000
Br	-2.677555000	3.703492000	1.471959000
Br	-0.264657000	1.392580000	0.865446000
O	-1.370163000	6.317920000	2.045192000
O	2.396351000	2.710642000	1.096634000



C	1.882289000	4.943974000	1.631944000
C	0.930792000	5.855302000	1.871627000
C	-0.515768000	5.499625000	1.830222000
C	1.541959000	3.528906000	1.311836000
C	-0.856085000	4.084665000	1.509447000
C	0.095432000	3.173330000	1.269915000

Cartesian coordinate for QI (in Å)

I	11.34789831724660	-1.51945984134358	9.27608749240645
I	5.18415393181739	-4.83124322234611	8.74637706517489
I	9.51337464524704	-2.69146625330675	12.25469596693273
I	7.02147755503089	-3.66391253692769	5.76750176345664
O	9.58602154491685	-2.33888640554971	6.87186980466656
O	6.94648151045126	-4.01269425730527	11.15050487518255
C	7.00781011589777	-3.84612892327232	8.80272810943721
C	8.98622438107133	-2.71901738107558	7.84437360722771
C	8.85792825234695	-2.93117085985107	10.30219901031118
C	7.54683263484628	-3.63317705179889	10.17808567653792
C	7.67552462938688	-3.42208804283625	7.72023018144272
C	9.52497248174071	-2.50605522438677	9.21964644722342



References

1. B. E. G. Lucier, A. R. Reidel and R. W. Schurko, Multinuclear solid-state NMR of square-planar platinum complexes — Cisplatin and related systems, *Canadian Journal of Chemistry*, 2011, **89**, 919-937.
2. M.-H. Thibault, B. E. G. Lucier, R. W. Schurko and F.-G. Fontaine, Synthesis and solid-state characterization of platinum complexes with hexadentate amino- and iminophosphine ligands, *Dalton Transactions*, 2009, DOI: 10.1039/B907737E, 7701-7716.
3. B. A. Demko and R. E. Wasylishen, Comparing Main Group and Transition-Metal Square-Planar Complexes of the Diselenoimidodiphosphinate Anion: A Solid-State NMR Investigation of M[N(iPr₂PSe)₂]₂ (M = Se, Te; Pd, Pt), *Inorganic Chemistry*, 2008, **47**, 2786-2797.
4. E. Kuzniak, J. Hooper, M. Srebro-Hooper, J. Kobylarczyk, M. Dziurka, B. Musielak, D. Pinkowicz, J. Raya, S. Ferlay and R. Podgajny, A concerted evolution of supramolecular interactions in a {cation; metal complex; π-acid; solvent} anion-π system, *Inorganic Chemistry Frontiers*, 2020, **7**, 1851-1863.
5. D. Sundholm, H. Fliegl and R. J. F. Berger, Calculations of magnetically induced current densities: theory and applications, *WIREs Computational Molecular Science*, 2016, **6**, 639-678.

